5-2010

Isolation and Identification of the Siderophore "Vicibactin" Produced by *Rhizobium leguminosarum* ATCC 14479.

William H. Wright IV
East Tennessee State University

Isolation and Identification of the Siderophore "Vicibactin" Produced by *Rhizobium leguminosarum* ATCC 14479

A thesis

presented to

the faculty of the Department of Health Sciences

East Tennessee State University

In partial fulfillment

of the requirements for the degree

Master of Science in Biology

---

by

William H. Wright IV

May 2010

Dr. Ranjan Chakraborty, Chair

Dr. Bert Lampson

Dr. Foster Levy

Keywords: *Rhizobium leguminosarum* ATCC 14479, siderophore, vicibactin

ABSTRACT

Isolation and Identification of the Siderophore "Vicibactin" Produced by *Rhizobium leguminosarum* ATCC 14479

by

William Wright

Siderophores are small, iron chelating molecules produced by many bacteria to help meet the iron requirements of the cell. Multiple metabolic functions require iron as it serves as a cofactor in many enzymes and cellular processes. However, in the presence of oxygen and at physiologic pH, iron forms insoluble ferric complexes that cause the nutrient to be unavailable to bacterial cells. Siderophores alleviate this limitation by chelating the ferric iron, rendering it soluble and available for uptake. One group of microorganisms known for their ability to produce siderophores is the rhizobia. These bacteria are characterized both by their formation of symbiotic relationships with leguminous plants and their ability to fix atmospheric nitrogen. *Rhizobium leguminosarum* ATCC 14479, which infects the red clover *Trifolium pratense*, was found to produce a trihydroxamate siderophore. Purification and chemical characterization identified this siderophore as Vicibactin that has been found to be produced by other rhizobial strains.

ACKNOWLEDGEMENTS

I would like first to thank my committee chair and mentor, Dr. Ranjan Chakraborty. Without all his guidance, patience, and especially his enthusiasm, I never could have made it this far. I thank my committee members Dr. Bert Lampson and Dr. Foster Levy for their comments and critical review of my thesis. I also am very grateful of Mr. James Little for the time he took in both analyzing my samples and teaching me to interpret the results. I wish to thank Mr. Ralph Coffman and Mrs. Robin Grindstaff for all their help within the labs. Many, many thanks go to the entire Health Sciences department for accepting me into the program, encouraging me to keep going, and forgiving me when I made my mistakes. I am thoroughly grateful for the assistance I received from all the graduate and undergraduate students I had the opportunity to work beside in the lab. Tom Barber, Beth Presswood, Ada Reynolds, David Hammond, Ralitsa Borisova, your companionship and support throughout was very much appreciated.

Lastly, I would like to thank my family for their support and understanding throughout this adventure. Most especially I want to thank to my wife Stacey for all her help, support, and love these past years. I would not be here now if it were not for her.

CONTENTS

LIST OF TABLES

LIST OF FIGURES

CHAPTER 1

INTRODUCTION

Iron, Its Availability and Uses

With the exception of a few species belonging to the *Borrelia*, *Lactobacillus* and *Streptococcus* genera, all organisms require iron (Storey et al. 2006). Physiologically iron acts as the catalytic center for a number of enzymes, particularly those involved in reduction-oxidation reactions such as the cytochromes used during cellular respiration as well as catalase and superoxide dismutase both of which are responsible for neutralizing toxic oxygen radicals in organisms inhabiting aerobic environments (Egli 2003). Iron has also been found acting as the terminal electron acceptor in a number of anaerobic and facultative bacteria, being reduced from ferric (Fe^{3+}) iron to its ferrous (Fe^{2+}) state. Conversely, some specialist bacteria such as *Acidithiobacillus ferrooxidans* (previously *Thiobacillus ferrooxidans*) have been found to use ferrous iron as a source of energy by oxidizing it to ferric iron (Chi et al. 2007).

Iron is the fourth most abundant element in the earth's crust and the second most common metal following oxygen, silicon, and aluminum respectively. Despite its relative abundance and metabolic value to most organisms, it can be a difficult nutrient to obtain. This is because when it is found in aerobic conditions and at neutral or physiologic pH, iron is oxidized to its ferric state and easily forms insoluble oxyhydroxides and other complexes that render it unavailable for metabolic use. In fact, the amount of available ferric iron in an external environment has been calculated at roughly 10^{-18} M. This limitation can be a serious threat to bacteria, most of which must maintain an internal iron concentration of around 10^{-6} M to survive. The situation

becomes more dire for pathogenic bacteria as mammalian hosts have iron sequestering mechanisms that lower the available iron concentration to 10^{-24} M (Raymond et al. 2003). Therefore, the acquisition of iron is a major concern for most living organisms. Many microorganisms have been found to react to iron limitation by secreting iron-complexing organic compounds that have a high affinity for iron. These molecules, known as siderophores, are responsible for scavenging any ferric iron that may be present in the surrounding environment for use by the cell.

Regulation of Iron Uptake Mechanisms

Uptake of iron is a tightly regulated system because iron, in both ferrous and ferric forms, can act catalytically to generate hydroxyl radicals (Guerinot 1994). Called the "Fenton Reaction", ferrous iron reacts with H_2O_2 (a normal metabolite in aerobic organisms) to form hydroxyl radicals. These radicals are potent oxidizing agents that can damage critical molecules found in living cells such as sugars, amino acids, phospholipids, DNA bases, and organic acids (Das et al. 2007). Many bacteria such as *Escherichia coli* control this problem by iron-regulating siderophore production using a repressor that is termed the 'Fur' (ferric uptake regulator) repressor (Hunt et al. 1994). This repressor is considered a key regulator for the expression of genes involved in iron transport and has been characterized in many Gram-negative and recently Gram-positive bacteria (Loprasert et al. 1999). There are over 90 genes that Fur acts as a transcriptional repressor for and many of these are involved in the biosynthesis and uptake of siderophores (Wexler et al. 2003).

In high iron environments, ferrous iron is abundant within the cell. Repression of iron uptake occurs when iron binds to inactive Fur proteins to form a complex that acts as the active transcription repressor (i.e. iron acts as a co-repressor). The repressor then binds to a conserved region of DNA near a promoter sequence known as the "Fur box", which blocks transcription of the gene. Fur has also been found to be an important global regulator. Aside from siderophore biosynthesis and uptake, fur regulates expression of virulence factor genes, oxidative stress protective genes, and pH stress genes (Loprasert et al. 1999). In bacteria with multiple siderophore systems additional regulation methods control the expression of genes for each system independently. Many bacteria use alternative sigma factors or activators for additional regulation (Meneely 2007).

Siderophores

In general, siderophores are low molecular weight compounds that can chelate ferric iron from many insoluble compounds in the environment. Ranging in size from 500 – 1500 daltons, they are synthesized by many microbes when growing under low iron conditions.

Siderophores can be divided into three main classes depending on the chemical nature of the functional group or groups used for Fe(III) coordination. These classes are the catecholates (*sensu stricto*, catecholates and phenolates; better termed as "aryl caps"), hydroxamates and the (α-hydroxy-)carboxylates (Miethke and Marahiel 2007). A fourth group, designated as "Mixed type", is comprised of those siderophore that use a combination of any of the above types to chelate iron. Examples of each siderophore class with the iron binding functional groups highlighted are shown in Figure

1. Fungi, bacteria, and plants are all known to have representatives capable of producing siderophores.

The hydroxamate family of siderophores is in some respects the classical variety of siderophore as ferrichrome was the first member of the series to be recognized as an iron transporting natural product from microbial sources (Neilands 1984). As stated above, the hydroxamate family is characterized by the use of one or more hydroxamic acid groups derived from amines such as lysine or ornithine to bind ferric iron (Patel and Walsh 2001). Several of these siderophores including exochelin, aerobactin, rhizobactin 1021, schizokinen, and alcaligin use two hydroxamate groups to bind iron. These are known as dihydroxamate siderophores and are noted to be produced by both gram-positive (ex: exochelin) and gram-negative (ex: alcaligin) bacteria. They are also produced by both opportunistic pathogens of mammalian hosts (ex: aerobactin) and soil-dwelling plant symbionts (rhizobactin 1021 and schizokinen) (Crosa et al. 2004).

The catecholate, or catechol type, siderophores are the second most common siderophore class aside from the fact that they have thus far only been found to be produced by bacteria (Dave et al. 2006). They have been found to contain either a mono- or dihydroxybenzoic acid residue that is used to chelate ferric iron and is derived from dihydroxybenzoic acid (Fischbach and Walsh 2006). The best studied example of a catechol type siderophore is enterobactin, sometimes called enterochelin, produced by *E. coli* (O'Brien and Gibson 1970).

The carboxylate family of siderophores is comprised of those that rely solely on the oxygen donor atoms of hydroxyl and carboxyl functional groups as donor groups to bind ferric iron (Drechsel et al. 1995). Since the discovery in 1985 of rhizobactin DM4

as the first representative of the carboxylate class of siderophores, they have since been found to be the only siderophores to be produced across all three domains; *Bacteria*, *Archaea*, and *Eukarya* (Dave et al. 2006). Examples of other siderophores belonging to this group include staphyloferrin A and B from *Staphylococci*, vibrioferrin from *Vibrio parahaemolyticus*, fungal rhizoferrin from the *Mucorale* fungi, and bacterial rhizoferrin produced by *Ralstonia pickettii*.

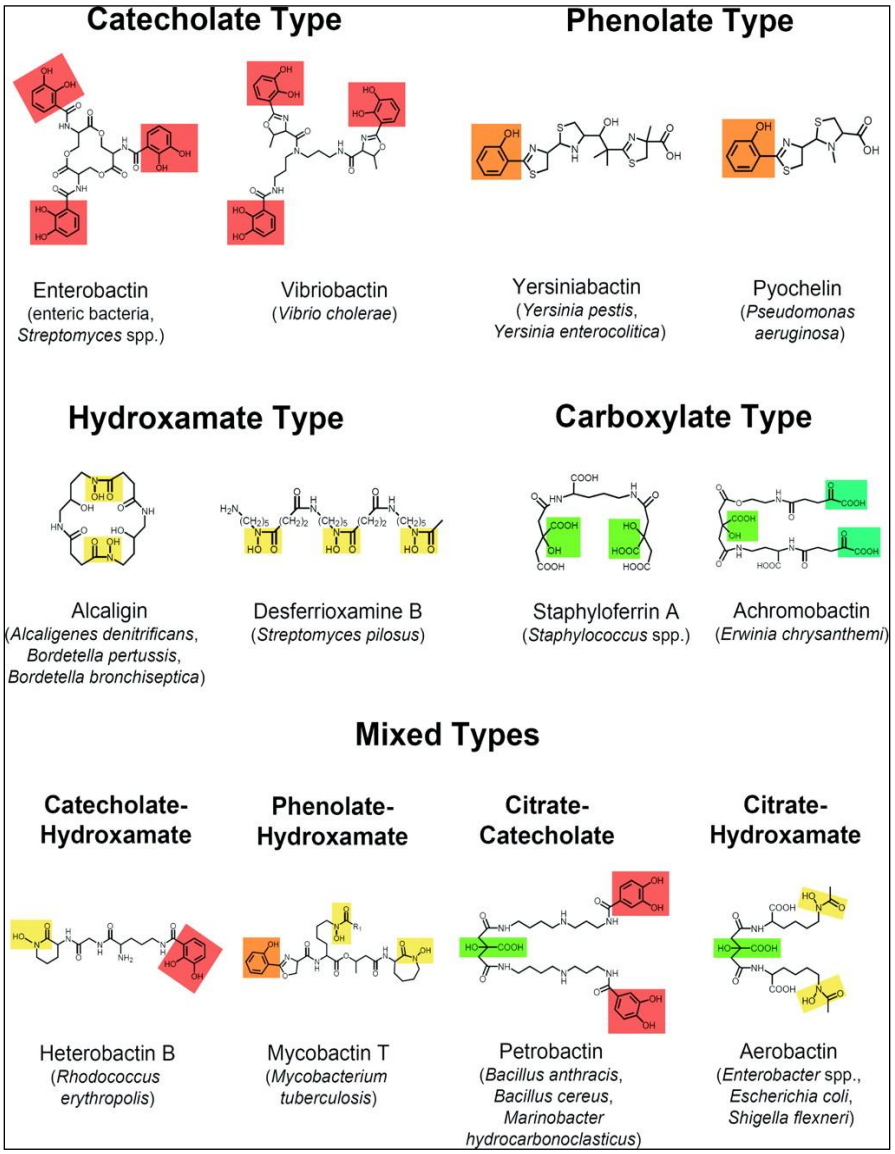

Figure 1: Examples of each siderophore class. Note that the phenolate type siderophore is a sub-category of the catecholate family (Miethke and Marahiel 2007).

The binding strength of siderophores varies depending on the specific molecule in question but in general those belonging to the carboxylate group are weaker iron chelators than the hydroxamates that in turn tend to be weaker than the catecholates. In fact, the complex formation constants (K_f) of siderophores range up to $K_f = 10^{52}$ for enterobactin (ideal tricatecholate siderophore); 10^{30} for trihydroxamates; 10^{23} for mixed dihydroxamate/carboxylates (aerobactin); and 10^{21} for pure carboxylates (rhizoferrin) (Drechsel and Jung 1988). Typically, a lower K_f indicates that a particular siderophore is a relatively weaker iron chelator than one with a higher K_f. However, the above values assume that the ligand is fully deprotonated. Depending upon pH of the environment, this is not always the case. Because protonation of the donor atoms is a competitive reaction to metal chelation, the pKa values of the donor groups have to be considered when evaluating the siderophores in effectiveness of iron complexation. Catecholate siderophores have pKa values from 6.5 to 8 for the dissociation of the first hydrogen and about 11.5 for the second hydrogen from the catecholic hydroxyl groups. Hydroxamates show pKa values from 8 to 9. The pKa values of carboxylates range from 3.5 to 5 making them efficient siderophores under lower-pH conditions at which catecholates and hydroxamates are still fully protonated (Miethke and Marahiel 2007).

Uptake of Ferric-Siderophore Complexes

Siderophores are produced and secreted by bacteria into the surrounding environment in order to make insoluble ferric iron polymers available for metabolic use by the cell. After the secreted apo-siderophore (iron-free siderophore) encounters and binds iron, the ferric-siderophore complex must be selectively transported back into the bacterium. Because concentrations of free iron inside the cell are much higher than the

concentration of available iron outside the cell, it is not possible to transport ferric iron into the cell through simple diffusion. Therefore, transport of the ferric-siderophore complex requires a specific, high-affinity, outer membrane receptor protein (OMRP) (Clement et al. 2004). Examples of these outer membrane receptors include the ferric enterobactin transporter, FepA, the ferrichrome transporter, FhuA, the transport protein for ferric dicitrate, FecA, and the ferric pyoverdine transporter, FpvA (Storey 2005). Once binding and passage through the outer membrane receptor has occurred, a common mode of transport across the periplasm, through the inner membrane, and into the cytoplasm is seen.

The model in Figure 2 below illustrates the route of complex transport currently believed to be used by Gram-negative bacteria. First, the ferric-siderophore complex binds to a specific outer membrane receptor. Once bound, the receptor is energized by a TonB complex and induced to transport the siderophore into the periplasm by the removal of a "plug" region within the receptor (Chakraborty et al. 2003, Raymond et al. 2003). In the example below, iron-bound ferrichrome is transported across the outer membrane via the protein FhuA. Next, a periplasmic binding protein binds to the siderophore complex and shuttles it to an ATP dependent ABC-type transporter found on the cell's inner membrane. The ABC-type transporter then undergoes ATP hydrolysis that allows transport of the complex into the cell's cytoplasm (Raymond et al. 2003).

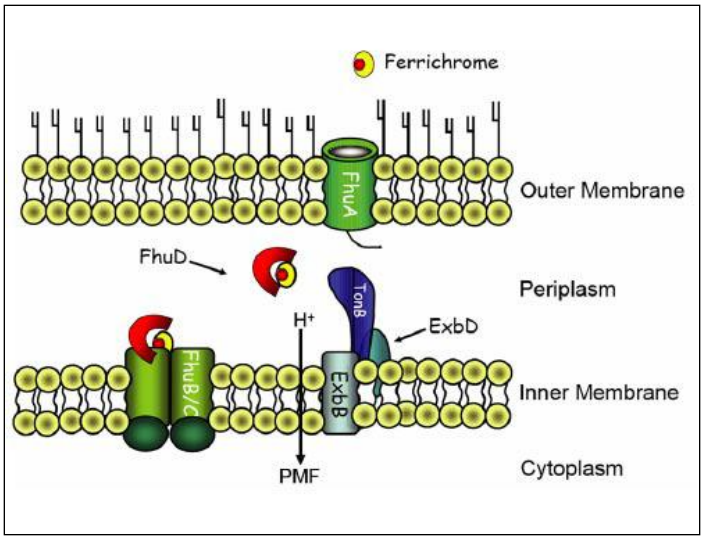

Figure 2. The ferric-siderophore uptake system of the hydroxamate siderophore, Ferrichrome. FhuA= specific outer membrane receptor for ferric-siderophore complex, FhuD = periplasmic binding protein, FhuB/C = ABC type transporter (Pawelek et al. 2006)

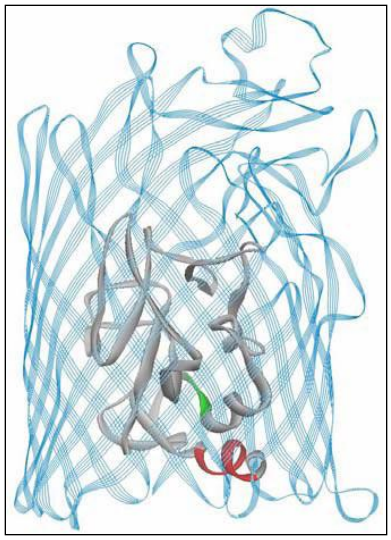

Figure 3. Crystallized structure of FhuA. The N-terminal "lock" region (solid gray ribbon) of these transporters is folded into the protein's β-barrel (solid blue ribbon). (adapted from Kim et al. 2007)

The Rhizobia

The rhizobia are an ecologically important paraphyletic grouping of soil bacteria generally classified based on their ability to infect and nodulate the roots of leguminous plants. Currently, the rhizobia are made up of 76 species found within 13 genera. Most of these bacterial species are in the *Rhizobiacae* family and are in either the *Rhizobium, Mesorhizobium, Ensifer* (formally *Sinorhizobium*), or *Bradyrhizobium* genera (Weir 2009). While each strain, species, genera, or family differs in which legumes they are capable of nodulating, they each form symbiotic relationships with the plant whose roots they have infected. Further details on this symbiotic relationship are covered later. Shared characteristics of the group include that they are all aerobic, gram-negative bacilli. They are motile in their free-living form and do not form endospores. The morphology of most rhizobia also includes an exopolysaccharide layer that is believed to assist in attachment to host plant root hairs. The optimal temperature for growth of these bacteria

is 25 – 30 °C and the favored carbon source is mannitol (Bergerson 1961). The rhizobia have also been found to have extremely large genomes. At approximately eight megabase pairs in length, rhizobial genomes are almost double that of *E. coli* and can differ by as much as 50% between two species (Johnston 2004). Many of these genes were indicated to be involved in the scavenging of nutrients upon genome sequencing of *R. leguminosarum* biovar *viciae* 3841 (Young et al. 2006). This provides the rhizobia with a competitive advantage by allowing them access to a wide range of nutrients for use in a wide range of metabolic functions.

Rhizobial Iron Regulation

Generally, each of the rhizobial species is capable of producing at least one siderophore. However, it is also true that in some genera such as *Bradyrhizobium* siderophore production is much less widespread. Examples of some rhizobial siderophores are the trihydroxamate vicibactin that was first isolated from *R. leguminosarum* (Dilworth et al. 1998); schizokinen and rhizobactin 1021, dihydroxamates isolated from *R. leguminosarum* (Storey et al. 2006) and *Sinorhizobium meliloti* (Persmark et al. 1993) respectively; and a carboxylate called rhizobactin found in *S. meliloti* (Smith et al. 1985). Like other organisms, iron uptake must be strictly regulated to avoid the toxic effects of the Fenton reaction as discussed earlier. However, whereas Fur is the major global regulator of iron in *E. coli, Pseudomonas aeruginosa* and *Bacillus subtilis*, its role in *Rhizobium* is either diminished, has an alternative function, or is absent altogether (Small et al. 2009). Instead, most rhizobia seem to use a protein that bears no similarity to Fur called RirA to control many of the iron regulated operons in *R.*

leguminosarum and *S. meliloti* (Todd et al. 2002; Viguier et al. 2005). Further, *B. japonicum*, has been found to use yet a third regulator deemed Irr (Hamza et al. 1998). Irr is unlike both Fur and RirA who negatively regulate (repress) the transcription of genes associated with ferric iron uptake when iron concentrations are high. Instead, Irr has been found to positively regulate these systems when under low iron conditions (Small et al. 2009). Irr has also been shown to be an iron-controlled transcriptional repressor of hemB in *B. japonicum*, which is involved in the synthesis of heme (Hamza et al. 1998). It can be clearly seen from this that there is no one model that can describe the regulation of iron uptake in all rhizobia (Johnston 2004).

Rhizobial Symbiosis and the Role of Iron

The symbiosis that rhizobia initiate with their respective host plant stems from the fact that all members of the rhizobia belong to a group of organisms termed diazotrophs, or organisms capable of fixing atmospheric nitrogen gas into a more biologically usable form such as ammonia. The bacteria infect and nodulate (Figure 4) the roots of the host plants via the root hairs and differentiate into bacteroids. Bacteroids are comprised of the intracellular forms of rhizobia with the functional nitrogen-fixing unit of the plant nodule (Nadler et al. 1990). It is in this form that the bacterial cells begin to fix inert nitrogen through the use of the nitrogenase enzyme complex of which iron is a major component (Loh and Stacey 2003). In return for supplying the host plant with a nitrogen source, the bacteria receive energy in the form of simple sugars, some nutrients, and a more stable, less competitive living environment. It has been estimated that this family alone is

accountable for the production of over $2x10^{13}$ grams of fixed nitrogen per year (Falkowski 1997).

The nitrogenase enzyme complex is a heterodimer consisting of iron-containing nitrogenase reductase and nitrogenase, which contains an iron-molybdenum cofactor where nitrogen reduction occurs (Johnston 2004). Previous research indicates that this enzyme complex accounts for 10 - 12% of the total protein weight of a bacteroid (Verma and Long 1983). Interestingly, although rhizobia are aerobic and therefore require oxygen for survival, the nitrogenase enzyme is oxygen labile and must be contained in an anaerobic environment within the aerobic cell. For this reason, leguminous plants produce a protein called leghemoglobin. Leghemoglobin is used in the root nodules to supply the rhizobial bacteroids with oxygen but also keeps free oxygen bound so that it is unable to interfere with the operation of the nitrogenase complex. Similar to hemoglobin found in blood, leghemoglobin contains iron and accounts for approximately 30% of the total soluble protein in the nodule (Verma and Long 1983). The reddish color seen in some nodules is due to an accumulation of leghemoglobin, which in turn is given its red color by the large amount of iron present in the protein (Hammond 2008).

Figure 4: Infection nodules formed by *R. leguminosarum* on clover roots.

Present Work

Rhizobium leguminosarum ATCC 14479 was obtained from the American Type Cell Culture and was investigated for the production of siderophore. First, it was determined that this strain produces a hydroxamate type siderophore under iron deficient conditions. Media and growth conditions were standardized for the production of this siderophore that was then purified using both manual column chromatography and high performance liquid chromatography (HPLC). Multiple chemical analyses were then performed on the purified compound to determine the chemical nature of the siderophore. Results indicate that the siderophore being produced by this strain is vicibactin, which is commonly produced by other rhizobial strains.

CHAPTER 2

MATERIALS AND METHODS

Bacterial Strain and Growth Conditions

Bacterial Strain

The bacterial strain used in this study was *Rhizobium leguminosarum* ATCC 14479 and was obtained from the American Type Culture Collection. It was isolated at Arlington Farms, VA and is most effective on the red clover, *Trifolium praetense*. Synonyms for this strain include USDA 2046, DSM 6040, and *Rhizobium trifolii* Dangeard 1926 (Ramı´rez-Bahena et al. 2008).

Congo Red Agar

The culture was maintained on a modified Mannitol Yeast Agar supplemented with Congo Red dye (Jadhav and Desai 1996). Bacteria belonging to the rhizobia are commonly grown on this agar because they typically do not absorb the dye as readily as other microorganisms which allows for the easy recognition of the presence of most contaminants (Kneen and Larue 1983). Figure 5 shows the difference in dye absorption exhibited by rhizobial (left) versus non-rhizobial (right) bacteria. The media contained (w/v): 1% mannitol, 0.05% K_2HPO_4, 0.02% $MgSO_4*7H_2O$, 0.01% NaCl, 0.1% yeast extract, and 3% Bacto-agar. The pH was adjusted to 6.8 using 6 M NaOH after which 1 ml of a 1% Congo red dye solution was added to the medium prior autoclaving (Hammond 2008). Colonies of *R. leguminosarum* ATCC 14479 developed on plates after 4 - 5 days incubation at 30°C.

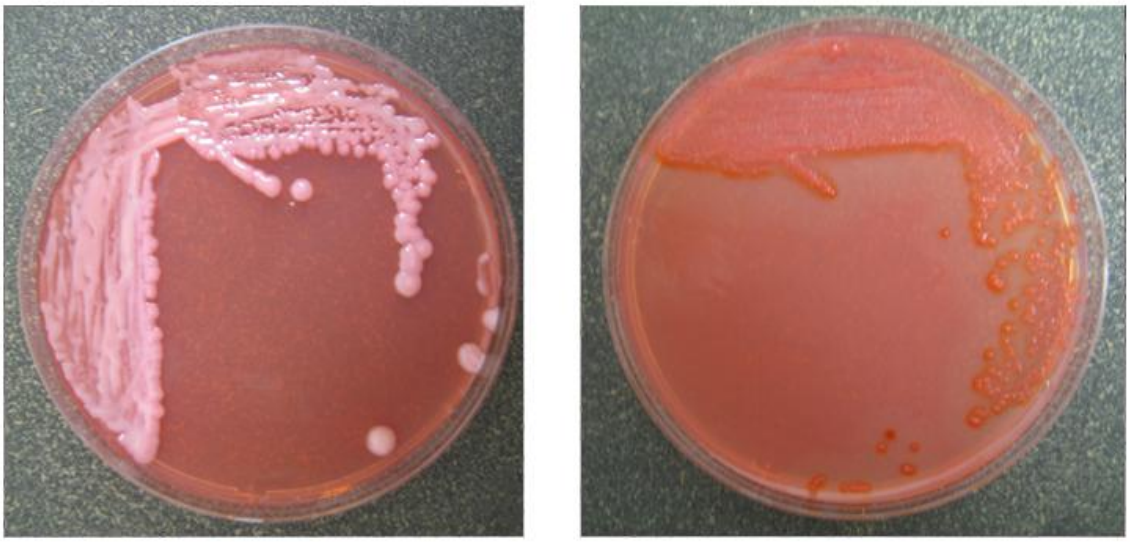

Figure 5: Rhizobial (left) and non-rhizobial (right) organisms grown on congo red agar. The rhizobia absorb the red dye much less readily than do non-rhizobial microbes.

MMW Minimal Media

As only iron-limiting conditions induce siderophore production, a defined minimal media had to be used. The defined media of Manhart and Wong (1979) was found to be successful in growing the strain and was modified by substituting dextrose in place of both arabinose and mannitol as the carbon source; glutamate in place of KNO_3 as a nitrogen source (Streeter 1985); and $FeCl_3 * 6H_2O$ was omitted from the vitamin solution as the presence of iron would repress the strain's need for siderophore production.

The media was termed modified Manhart and Wong media, "MMW" and had the following composition (w/v): 0.0764% K_2HPO_4, 0.1% KH_2PO_4, 0.15% Glutamate, 0.018% $MgSO_4$, 0.013% $CaSO_4*2H_2O$, and 0.6% Dextrose. Prior to being autoclaved, pH was adjusted to 6.8 using 6 M NaOH. After autoclaving, the media was cooled to room temperature and 1mL of filter sterilized, concentrated vitamin solution was added per liter of basal media. *R. leguminosarum* ATCC 14479 was found to be resistant to penicillin, allowing the addition of this antibiotic to media to reduce risk of

contamination by other microorganisms. Filter sterilized 100 mg/mL aqueous solution of penicillin was added to the cooled media to a final concentration of 50μg/mL. Total media composition can be seen below on Table 1. In addition to the use of a minimal media, all glassware used for either media storage or for culture growth were treated with concentrated HNO_3 for a minimum of 1 hour in order to minimize the amount of contaminant iron. All glassware was then thoroughly rinsed with ddH_2O.

Table 1: MMW Media Composition

MMW Basal Media	
Component	g/L
K_2HPO_4	0.764
KH_2PO_4	1.0
Glutamate	1.5
$MgSO_4$	0.18
$CaSO_4*2H_2O$	0.13
Dextrose	6.0

Basal media was autoclaved and allowed to cool to room temperature before the addition of 1mL concentrated vitamin/trace metal solution and 500μL of 100mg/mL penicillin per 1L media.

Concentrated Vitamin and Trace Metal Solution (1000x)	
Component	mg per 100 mL ddH_2O
H_3BO_3	145
$CuSO_4*5H_2O$	4.37
$MnCl_2*4H_2O$	4.3
$ZnSO_4*7H_2O$	108
$Na_2MoO_4*2H_2O$	250
$CoCl_2*6H_2O$	10
$Na_2EDTA*2H_2O$	550
Riboflavin	10
ρ-aminobenzoic Acid	10
Nicotinic Acid	10
Biotin	12
Thiamine HCl	40
Pyridoxine HCl	10
Calcium Panthenate	50
Inositol	50
Vitamin B12	10

Preparation of Inoculum (Seed Culture)

Seed cultures were prepared from fresh, isolated colonies grown on congo red agar plates. *R. leguminosarum* ATCC 14479 was grown in MMW broth on a rotary shaker until it reached mid log phase (approx. 72 hours) and was then used as inoculum.

Detection of Siderophore Production

Chrome Azurol Sulfonate (CAS) Assay

A universal chemical assay for the general detection of siderophores was used to first determine if *R. leguminosarum* ATCC 14479 produced a siderophore. The CAS assay (Schwyn and Neilands 1987) is based on all siderophores' strong ability to chelate ferric iron. The agar contains Chrome Azurol S (CAS) dye that, when bound to ferric iron, is blue in color. A color change from blue to yellow/orange occurs when iron is stripped from the CAS dye. *R. leguminosarum* ATCC 14479 was grown in iron-free, MMW media for 96 hours at 30°C on a rotary shaker. Supernatant was collected by centrifugation of culture at 14,000 rpm for 30 min. A #2 cork borer was used to cut wells into a CAS plate into which 65 μL of each culture supernatant was pipetted. Sterile media was added to a well to act as a negative control. The plate was then incubated at room temperature overnight. Siderophore production was indicated by the formation of an orange halo around a well. Size and color intensity of these halos is directly related to the amount of siderophore produced and its relative chelating strength.

Atkin's Assay for Detection of Hydroxamate-Type Siderophores

Once siderophore production was determined via the CAS assay, additional colorimetric tests were used to determine the class of the siderophore(s). Hydroxamate-type siderophores can be detected through the use of the iron-perchlorate assay (Atkin et al. 1970). Culture supernatants were collected as previously described and 0.5 ml supernatant added to 2.5 ml of a solution containing 5 mM $Fe(ClO_4)_3$ in 0.1 M $HClO_4$. Once the supernatant is added, the reaction is allowed to incubate at room temperature for

approximately 5 minutes. A positive result causes a wine color to form. The intensity of the resultant wine color varies based on the amount of siderophore present in the sample. Absorbance is measured at 480 nm and is compared against a colorless blank that is made up of uninoculated media mixed with reagent.

Arnow's Assay for Detection of Catechol-Type Siderophores

The second colorimetric assay used to determine siderophore type was the Arnow's assay (Arnow 1937)) that detects the presence of catecholate functional groups by producing a yellow colored solution. The procedure for this assay is performed by adding each of the reagents in the following sequence: 1 ml culture supernatant, 1 mL 0.5 M HCl, 1 mL nitrite-molybdate reagent (prepared by dissolving 10 g sodium nitrite and 10 g sodium molybdate in 100 ml ddH2O), and 1 mL 1 M NaOH. This mixture is then allowed to incubate for 5 minutes at room temperature. Finally, absorbance at 500 nm is measured and again compared with the absorbance of an uninoculated blank. The blank remained colorless after addition of reagents.

Siderophore Detection Using Thin Layer Chromatography (TLC)

Normal phase TLC was used to detect the presence of siderophore in concentrated fraction samples (see later sections). Concentrated fractions were spotted one inch from the bottom of 10 x 20 or 5 x 10 silica gel plates and allowed to dry. The plates were then placed in a sealed glass chamber containing a n-butanol:acetic acid:dH2O (12:3:5) solvent and allowed to run until the solvent front came within approximately one inch of the top of the plate. These plates were then dried and developed by being sprayed with

0.1 M $FeCl_3$ in 0.1 N HCl and again allowed to dry (Storey 2005). As the solvent moves up the gel plate, it separates molecules based on that molecule's polarity. Using this system, polar compounds have a stronger binding potential with the silica gel than with the solvent. This causes more polar compounds to not move as high up the plate as less polar molecules (Boyer 2000). After being sprayed with the developing solution, hydroxamate-type siderophores appear as wine colored spots where as catechol-type siderophores result in a dark gray spot.

Optimization of Siderophore Production

Optimization of Incubation Time

Siderophore production is influenced by the stage of the growth phase of the culture being tested. Two methods were used to evaluate the incubation time needed by *R. leguminosarum* ATCC 14479 to reach maximum siderophore production. Initially, cultures were grown in 50 mL volumes of MMW_{pen50} and analyzed via a CAS assay. A sample (1 mL) was removed from the culture every 24 hours for 5 days and the supernatant collected by centrifugation at 13,000 rpm for 30 minutes. These samples were kept at 4 °C until all samples were collected and the CAS assay was conducted as previously described. Plates were incubated at room temperature for 24 hours after which each halo's diameter was measured. After identification of the siderophore, the effect of incubation time on siderophore production was re-evaluated using the Atkin's method as previously described. For this method, one liter of MMW_{pen50} in a 2.8 L fernbach flask was inoculated with 10 mL of seed culture. Starting at 24 hours and every 12 hours thereafter, a 1 mL aliquot was removed and growth measured at OD_{600} nm.

Culture supernatant was collected by centrifugation at 13,000 rpm for 30 minutes and evaluated via the Atkin's assay at 450 nm, the published absorbance maximum for the identified siderophore.

Optimization of Iron Concentration

Siderophores are only produced by a cell under iron deficient conditions. However; it has been noted that a small concentration of iron is required for siderophore production. Further, while precautions are taken to eliminate iron from all glassware, it is still present as a manufacturing contaminant in several media components which was calculated to be at a concentration of 0.270 μM. To analyze the effect of various iron concentrations on siderophore production, cultures were grown in 50 mLs of MMW media supplemented with iron. Filter sterilized iron solution was added to each culture flask to reach the following μM concentrations: 0 (no added iron), 0.25, 0.5, 0.75, 1.0, 2.0, 5.0, 10.0, 20.0, 100.0. Another culture flask was brought to an iron concentration of -0.270 μM (absolute zero) by supplementing the media with 0.2 mM 2'2-dypyridyl which chelates ferrous iron and effectively renders it unavailable for cellular use. Cultures were incubated at 30°C for 100 hours after which supernatant was collected by centrifugation at 14,000 rpms for 30 minutes. Optical density at OD_{600} of both culture and supernatant was taken to measure growth and the remaining turbidity due to dissolved exopolysaccharide respectively. Siderophore production was measured via the Atkin's assay; however, the procedure had to be modified to include an ethanol precipitation step to remove exopolysaccharide. It was found that altering the media composition affected the amount of exopolysaccharide produced by the organism. The varying concentrations

of exopolysaccharide in the cultures caused erroneous assay results mainly in the form of false positives. In these cases, 100% ethanol was added to the media supernatant at a ratio of 2:1 and centrifuged at 13,200 rpm for 10 min to pellet the precipitated polysaccharide. This second supernatant can then be used in the Atkin's assay as described above and the OD_{450} results multiplied by 3 to correct for dilution.

Siderophore Purification

Batch Cultures

Large volumes of initial culture are needed to obtain enough of the purified siderophore for chemical characterization. To meet this requirement, 3 L of MMW_{pen50} media was inoculated with a 10 mL seed inoculum per liter. These cultures were grown for 96 hours at 30 °C on a rotary shaker operating at 200 rpm. Culture supernatant was obtained by centrifugation at 14,000 rpm for 30 minutes and collected into acid treated bottles. The relatively high centrifugation speed was needed to remove as much of the exopolysaccharide produced by this strain as possible.

Amberlite XAD-2 Column Chromatography

To begin the purification process, a 5 x 30 cm column packed with Amberlite XAD-2 that binds cyclic compounds was used. The column was prepared by suspending approximately 160g of XAD-2 in ddH_2O and letting it soak overnight at room temperature in order for the beads to fully absorb the water. After soaking, the prepared beads were packed into the column to a height of 8 cm, cleaned with three bed volumes (1 bed volume = ~160mLs) of methanol, and equilibrated with four bed volumes of

ddH_2O. In order to make siderophores less soluble in water, collected supernatant was acidified to pH 2.0 using 6M HCl. Each liter of acidified supernatant was then passed through the prepared column and all flow-through was collected. Due to the viscosity of the supernatants and to reduce clogging of the column, washing and elution of the column was performed after each liter of acidified supernatant was run. After each liter of supernatant was run and flow-through collected, the column was washed with two bed volumes of ddH_2O and collected in a separate bottle. Elution of the column was performed by passing approximately 400 mL of methanol through the column. This elution was collected in approximately eight 50 mL fractions. Following elution, the column was washed with four more bed volumes of methanol and re-equilibrated with four bed volumes of ddH_2O to ready the column for the next liter of supernatant. The flow-through from each of these two steps was also collected separately. All collected fractions, washes, and re-equilibration flow-through were then tested for the presence of siderophore using the CAS assay. Fractions that tested positive were combined and collected in a fresh, acid treated bottle. After collection of all siderophore containing fractions, they were concentrated using a Labconco CentriVap Centrifugal Concentrator. Collected fractions were separated into 30 mL aliquots and placed into 50 mL tubes. These were placed into the concentrator and evaporated under vacuum at 40 °C. The concentrated, dry pellet was resuspended in 5 mLs of methanol and centrifuged at 8500 rpm to remove precipitates that formed due to concentration. This supernatant was then loaded on a Sephadex LH-20 column for separation.

Sephadex LH-20 Column Chromatography

Further purification was accomplished by running the concentrated XAD-2 fractions through a Sephadex LH-20 column that separates compounds according to their hydrophobicity as well as by molecular weight. This column was prepared by suspending 25 g of LH-20 material in methanol and deaerating via gentle shaking for roughly 20 minutes. Following this treatment, the material was packed into a 1.5 x 50 cm column to a depth of 45 cm. It was then equilibrated with three bed volumes (1 bed volume = ~80mLs) of methanol and loaded with the concentrated sample. The column was run using methanol as the mobile phase. A total of 55 fractions were collected in 250 drop aliquots using a Bio-Rad Model 2110 fraction collector. These were then tested for the presence of siderophore using TLC as previously described and the concentrated XAD-2 sample as the positive control. Fractions (approximately 10mLs) found to contain siderophore were combined into 15mL tubes and evaporated at 40°C in the centrifugal concentrator until dry. The sample was then stored at –20°C until needed for further purification.

High Pressure Liquid Chromatography (HPLC)

Final purification of the concentrated siderophore samples was accomplished using a BioRad Biologic Duoflow HPLC system. A Waters 7.8 mm x 300 mm Novapak HR C_{18} hydrophobic column was used as the stationary phase. Filtered, deaerated ddH_2O and filtered 100% methanol were used as the mobile phases. The dried LH-20 purified samples were redissolved in 10 mLs ddH_2O and syringe-filtered into a 15 ml tube using a 0.45 μm filter. The UV detector on the HPLC system was set to 280 nm and the column

was equilibrated with three bed volumes ddH_20 before use. Approximately 2 mL of sample was injected onto the column in three consecutive 0.7 mL injections. Several preliminary runs were conducted to establish the methanol gradient at which the siderophore eluted from the column. Multiple programs were fashioned and refined to best separate the siderophore from impurities contained within the sample. A chromatogram was created at the conclusion of each program. Fractions showing peaks on the chromatograms were then tested for the presence of siderophore using TLC. All fractions testing positive for siderophore were combined and concentrated for further analysis.

Chemical Characterization of Purified Siderophore

Following collection of the purified siderophore sample, various chemical analyses were conducted to chemically characterize the siderophore and to determine its structure.

Spectral Scan Analysis

Purified siderophore samples were subjected to a spectral scan (300 - 700 nm) to determine whether the siderophore samples were dihydroxamate or trihydroxamate (Jalal and van der Helm 1991). Samples were prepared according to the Atkin's method, except that only 30 μL (rather than 0.5 mL) of concentrated siderophore sample was used (Storey 2005). An appropriate amount of ddH_2O was added to bring the sample volume to 0.5 ml. At pH 2.0, ferric trihydroxamate siderophores show an absorbance maxima centered in the 420-440 nm range, whereas ferric mono- and dihydroxamates absorb maximally in the 500-520 nm range (Jalal and van der Helm 1991).

Electrospray Mass Spectroscopy

Samples were analyzed by electrospray mass spectrometry using a Waters LCT-TOF (orthogonal acceleration time-of-flight mass spectrometer) equipped with a Hamilton syringe pump and Hewlett Packard HPLC-UV-VIS system. Both ferriated (iron-complexed) and deferriated (non-complexed) forms of the dried siderophore samples were provided for analyses to determine both the molecular weight and structure of the compounds.

Each sample was first dissolved in methanol and 5 μL injected onto a Hewlett Packard Hypersil column (4.6 x 100mm, ODS, PN 7991800-554) column. Solvent A was prepared by adding 30 mL of acetonitrile to an aqueous solution of 2.5 mM ammonium acetate. Solvent B was acetonitrile. 0.1 mL/min of 25 mM ammonium acetate in methanol was added post column between the diode array detector and the mass spectrometer source. Samples of the iron-complexes were dissolved in methanol then diluted to the appropriate concentration in 50/50 methanol/water for infusion. The samples were infused at a rate of 9 μL/min into the electrospray source and the data obtained in both positive and negative ion modes at sample cone voltages of 25, 75, and 150. The electrospray voltage was reduced below 3000 volts to get approximately 300 - 500 counts/sec for the metal ion complex of interest.

Accurate mass data for the compounds were obtained by infusing methanol solutions of the iron-free materials at 25 volts. Higher voltages (75 and 150 volts) were used to induce fragmentation of the molecules in order to gain sub-structural information. Approximately 10 – 30 μL of the solutions was dissolved in 4.5 mM ammonium acetate in 50/50 acetonitrile/water. Polypropylene glycol was added to use as the mass calibrant.

When the ionized samples are injected, the ions within are separated according to their mass per charge ratio (m/z). The ions then progress through a detector that calculates molecular weights of the ions/fragments present based on the trajectory and time-of-flight of each ion. A total of 10 measurements of 10 - 20 scans per determination were acquired and the results averaged for each sample.

The Waters MassLynx Elemental Composition Program was used to determine possible molecular formulae based on the ES/MS data. Standard deviation of the accurate mass measurements was approximately 2 ppm. In order not to exclude search candidates by employing too narrow of mass tolerance a search tolerance of 10 ppm was employed. Reasonable elements and the range of each element were chosen that are consistent for known classes of siderophores. The theoretical isotopic pattern (generated using the MassLynx Isotopic modeling Program) of the proposed formula from the Elemental Composition Program was compared to the observed pattern for further confirmation.

Nuclear Magnetic Resonance (NMR) Spectroscopy

The purified siderophore samples were also examined by 1H 1D NMR. The dried samples were dissolved in 1 mL of methanol-d4 for this analysis. The NMR spectra were collected in a 5-mm OD NMR tube on a JEOL Eclipse 600 MHz NMR spectrometer operating at ambient probe temperature. Final proton 1D NMR spectra were obtained by averaging 256 spectra using a pulse delay of 15 seconds. The residual proton resonance in methanol-d4 was used as the 1H chemical shift standard at 3.31 ppm (pentet).

Deuterium Exchange Analysis

Deuterium exchange analyses were conducted to further confirm the proposed structures. All three purified, deferriated siderophore samples were analyzed to determine the number of exchangeable protons on each of the compounds. Exchangeable protons are any hydrogen atoms bonded to either nitrogen or oxygen. For this analysis, these protons are exchanged with deuterium. Deuterium, or "heavy hydrogen", is composed of a hydrogen atom plus a neutron and has an atomic weight of 2 atomic mass unit (amu). Because hydrogen only has an atom mass of 1 amu, a molecule's MW increases by 1 for each instance in which a deuterium atom replaces an exchangeable proton. The number of exchangeable protons can be determined by comparing molecular weights for a given molecule both before and after the assay. This information can then provide insight into the structure of the examined molecule (Hemling et al. 1994, Lam and Ramanathan 2002). The samples were prepared by dissolving 4-8 μL of the sample/methanol solution described previously into 1 mL of 50:50 acetontrile-d3:deuterium oxide containing 5 μL of acetic acid-d4. The samples were then analyzed with the LCT-MS using both positive and negative electrospray ionization via infusion.

Amino Acid Analysis Using TLC

Purified siderophore samples were examined for their amino acid content to help confirm siderophore identity. The pure siderophore samples were acid hydrolyzed by combining them with an equal volume of 6 M HCl followed by autoclaving at 121°C for 6 hours. As vicibactin is composed of three ornithine residues, a standard was prepared by dissolving 1 mg of ornithine into 1mL ddH_2O. A volume of 3 μL of each hydrolyzed

sample and ornithine standard were spotted onto 20x20 TLC plates and run using a solvent system composed of acetonitrile: 0.1 M ammonium acetate (60:40). These plates were allowed to run until the solvent front reached approximately one inch from the top of plate. To color the amino acid spots, the plate was dried and developed by being sprayed with 0.5% (w/v) ninhydrin in ethanol followed by incubation at 55°C for 15 minutes (Storey et al. 2006).

CHAPTER 3

RESULTS

Initial Detection of Siderophore Production

The CAS assay was used for initial determination of siderophore production in *Rhizobium leguminosarum* ATCC 14479. Although characterization of siderophore class is not possible through this method, relative abundance and strength of the siderophore can be ascertained by the size of the halo and its color intensity respectively. Figure 6 shows that *R. leguminosarum* ATCC 14479 does produce a siderophore.

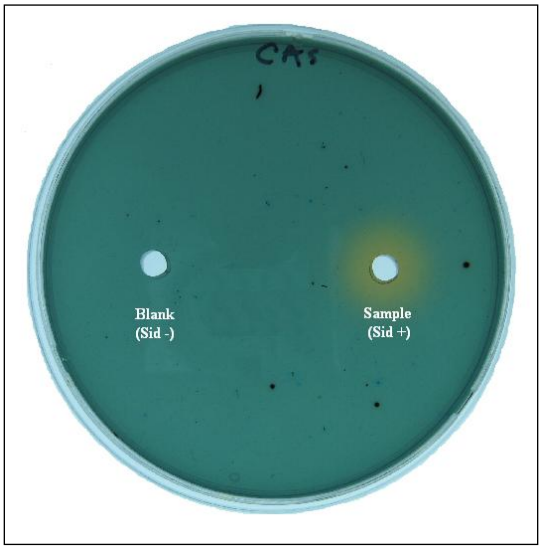

Figure 6: CAS assay for determination of siderophore production. Agar plate contains two bored wells. Blank well (left) shows no halo while the sample well (right) is surrounded by a yellow/orange halo indicating the presence of siderophore.

Initial Characterization of Siderophore

Once siderophore production was observed via the CAS assay, siderophore type was ascertained using the Atkin's and Arnow's assays. Culture supernatant was tested using both methods. Figure 7 shows the results of these tests. The Arnow's assay repeatedly tested negative for the presence of catechols. The Atkin's assay consistently tested positive, indicating that *Rhizobium leguminosarum* ATCC 14479 produces a hydroxamate type siderophore.

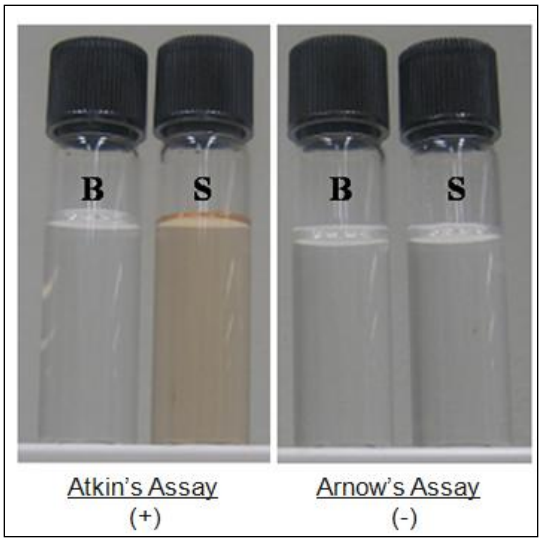

Figure 7: Results of the Atkin's and Arnow's Assays: blank (B), sample (S). The positive Atkin's result indicates a hydroxamate type siderophore.

Optimization of Siderophore Production

Optimization of Incubation Time

The CAS assay was initially used to determine the length of incubation time required for the maximum amount of siderophore production. The organism was grown in 50mL of MMW_{pen50}. A 1 mL sample of culture supernatant was collected every 24 hours for 5 days and kept at 4°C. Once all samples were collected, approximately 65 µL of each were transferred into wells cut into the CAS agar. The diameter of each siderophore halo was measured. These results can be seen in Table 2 and indicated that approximately 96 hours of incubation resulted in the greatest siderophore production.

Table 2: Effect of incubation time on CAS halo diameter

Incubation Time (hrs)	Halo Diameter (cm)
24	0
48	1.5
72	1.8
96	2.0
120	1.8

Once the siderophore was chemically identified, this experiment was repeated using the Atkin's assay to obtain more accurate data (Figure 8). Siderophore production was measured at 450 nm as this was the experimentally determined maximum absorbance (published max absorbance 445nm). Bacterial growth was also measured at OD_{600}. These results corresponded with the CAS assay results, indicating that maximum siderophore production did occur at approximately 96 hours incubation.

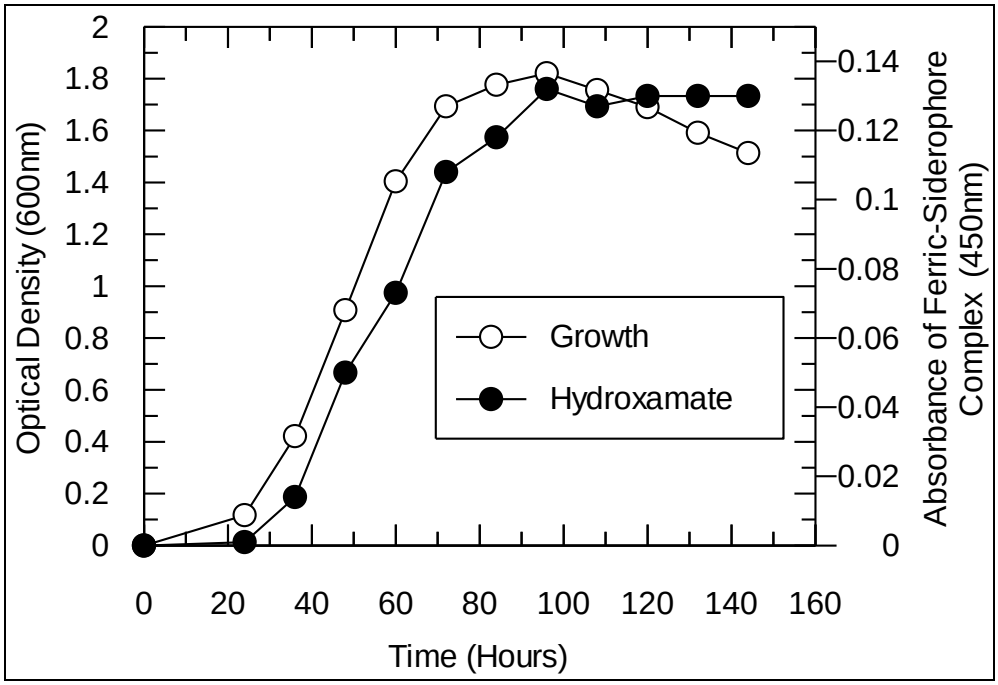

Figure 8: Growth and siderophore production over time of *Rhizobium leguminosarum* ATCC 14479.

Optimization of Iron Concentration

Siderophores are secondary metabolites, only being produced by cells when iron availability is limited and being down regulated when iron is in abundance. However; it has also been observed that small amounts of iron are actually required for siderophore production. Therefore, it was important to characterize the effect of iron concentration in the medium on siderophore production. *R. leguminosarum* ATCC 14479 was grown in MMW_{pen50} supplemented with various concentrations of ferric iron added as $FeCl_3$

solution. The strain was also grown in media supplemented with 0.2mM 2'2 dipyridyl to completely remove any iron that was present as a contaminant within the medium components (calculated at ~0.27μM). Figure 9 illustrates the results of this experiment and the classic biphasic relationship between iron concentration and siderophore production. The data (Table 3) were collected by performing the Atkin's assay on 96 hour culture supernatant, culture supernatant diluted with ddH_2O (1:2 ratio) and culture supernatant diluted with ethanol (1:2 ratio) to precipitate remaining bacterial polysaccharide. Both maximum growth and siderophore production were attained by supplementing 0.25 μM ferric iron to the medium (Figure 9). Higher iron concentrations led to a decrease in siderophore production. Bacterial growth, and consequently siderophore production, was negligible in the 2'2 dipyridyl supplemented medium. This is presumably due to the complete lack of iron, which would inhibit cellular metabolism and viability.

Table 3: Results of the effect of supplemented iron concentration on culture growth and siderophore production. The Atkin's assay was used on three different treatment samples: culture supernatant (S), 1:2 diluted culture supernatant in ddH_20 (DS), and 1:2 diluted culture supernatant in ethanol (EpS).

		Optical Density at 600nm (OD_{600})		**Atkin's Assay Absorbance at 450nm (OD_{450})**			**Dilution Correction (OD_{450} x 3)**	
Flask #	**Fe Conc. (μM)**	**Culture**	**Supernatant**	**Supernatant (S)**	**Diluted Supernatant (DS)**	**EtOH ppt. Supernatant (EpS)**	**DS x 3**	**EpS x 3**
1	-0.27	0.083	0.001	0.005	0.001	0	0.003	0
2	0	1.452	0.096	0.083	0.030	0.015	0.090	0.045
3	0.25	1.811	0.156	0.142	0.050	0.030	0.150	0.090
4	0.50	1.796	0.099	0.093	0.027	0.015	0.081	0.045
5	0.75	1.783	0.090	0.079	0.023	0.004	0.069	0.012
6	1.0	1.743	0.184	0.061	0.027	0	0.081	0
7	2.0	1.758	0.158	0.050	0.018	0	0.054	0
8	5.0	1.748	0.207	0.055	0.016	0	0.048	0
9	10	1.798	0.207	0.063	0.021	0	0.063	0
10	20	1.732	0.262	0.089	0.032	0	0.096	0
11	100	1.782	0.151	0.060	0.016	0	0.048	0

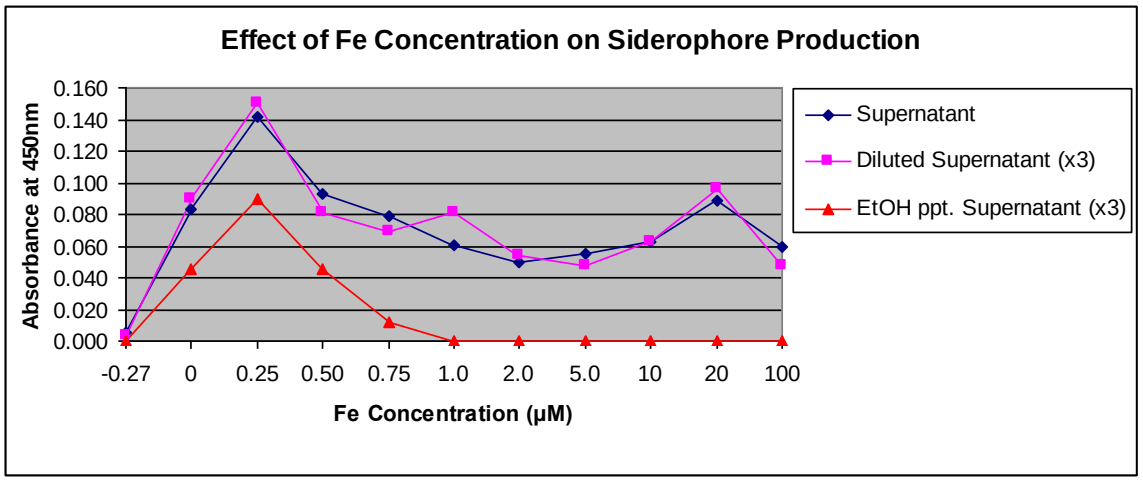

Figure 9: Effect of supplemented iron concentration on siderophore production. Absorbance is greater in the supernatant and diluted supernatant samples due to the presence of polysaccharide. True siderophore absorbance is better represented by the EtOH treated sample. Peak production for *R. leguminosarum* ATCC 14479 in all three samples is at 0.25 µM of supplemented $FeCl_3$.

Siderophore Purification

Amberlite XAD-2 Column Chromatography

R. leguminosarum ATCC 14479 was grown for 96-100 hours in 1L batch cultures of MMW_{pen50} in order to generate large amounts of siderophore. Three liters of cultures were grown and the culture supernatant was acidified to pH 2 prior to initial purification via Sephadex XAD-2 column chromatography. Fractions were collected in 50mL aliquots and each was tested for its siderophore content using CAS plates. In addition to testing eluted fractions, all flow through collected from column washes and equilibrations was also tested to ensure that all siderophore had been bound to the column material. The CAS halos (Figure 10) indicated that majority of siderophore eluted in fractions 4 - 7, although there appeared to be a small amount eluted in fraction eight as well. Maximum siderophore elution occurred in fractions five and six.

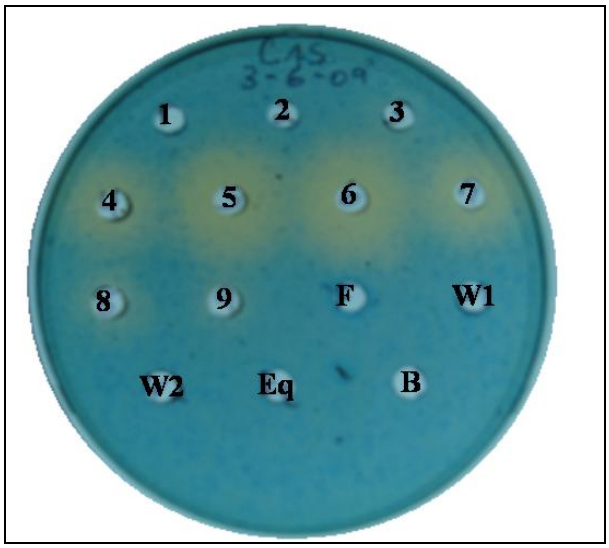

Figure 10: Amberlite XAD-2 fractions collected and tested using CAS asay. Yellow halos correspond to those fractions that contain siderophore. Fractions 1-9 numbered as shown. F: flow through, W1: ddH_2O wash, W2: methanol wash, Eq: ddH_2O equilibration, B: sterile ddH_2O blank

Sephadex LH-20 Column Chromatography

All XAD-2 fractions testing positive for siderophore content on CAS plates were combined, dried, and resuspended in 5 mL methanol. This was then centrifuged at 8500rpm for 30 min to remove precipitates. This concentrated sample was then further purified using Sephadex LH-20 column chromatography. A total of 55 fractions were collected in 250 drop aliquots. Each of these was tested for siderophore content via normal phase TLC. It was noticed at this point that there appeared to be two spots develop showing retention factors of 0.46 and 0.69 as can be seen in Figure 11. These spots developed in both the positive control (concentrated XAD-2 sample) and the LH-20 fractions 13 - 20. These spots were indicative of one of two possibilities; either each is a separate siderophore or one could be a degradation product of the siderophore that still retains the ability to chelate iron. Due to the gradual "smearing" that occurred between fractions 16 - 18, it was decided to combine fractions 13 - 19 rather than save them separately. These fractions were combined, dried, and resuspended in 10mL ddH_2O for final purification through HPLC.

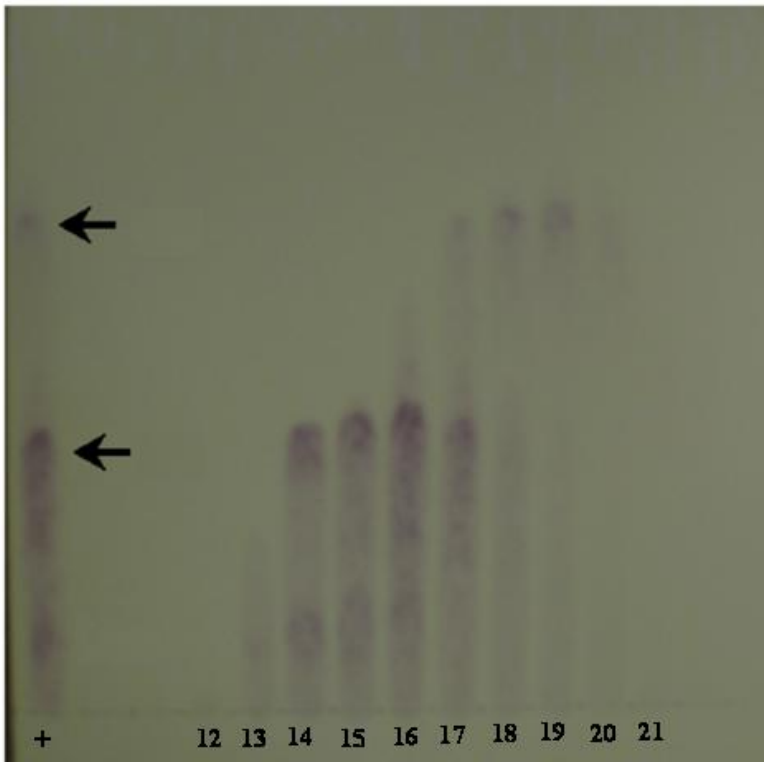

Figure 11: TLC results for Fractions 10 - 26 post Sephadex LH-20 column. "+" control arrows indicate that at least two iron-binding compounds were present in sample both before and after passing through the column.

High Pressure Liquid Chromatography (HPLC)

HPLC was used as the final purification step of the siderophore sample using distilled water as solvent A and methanol as solvent B. The siderophore positive LH-20 samples were loaded onto a Waters C_{18} hydrophobic HPLC column. Multiple programs and trials were run and continually refined in order to obtain good separation of peaks. TLC was used to test peak positive HPLC fractions after each trial was run. Previously, TLC had revealed the presence of two potential siderophores from the LH-20 samples. The TLC analysis now presented three potential siderophores as indicated by the presence of three distinct, wine colored spots eluting in differing fractions. These were labeled A, B, and C with each eluting into fractions 23, 28-29, and 35-36 respectively. Figure 12 shows the TLC plate from the initial HPLC run indicating three potential

siderophores. The HPLC program was continually refined and run for each of the three molecules until isolated peaks were obtained for each. After isolation of the three molecules was attained, each was dried via evaporation and the pure compounds weighed. Figure 13 shows the final HPLC chromatograms, dry weights, and the methanol concentrations at which each pure compound eluted for molecules A, B, and C.

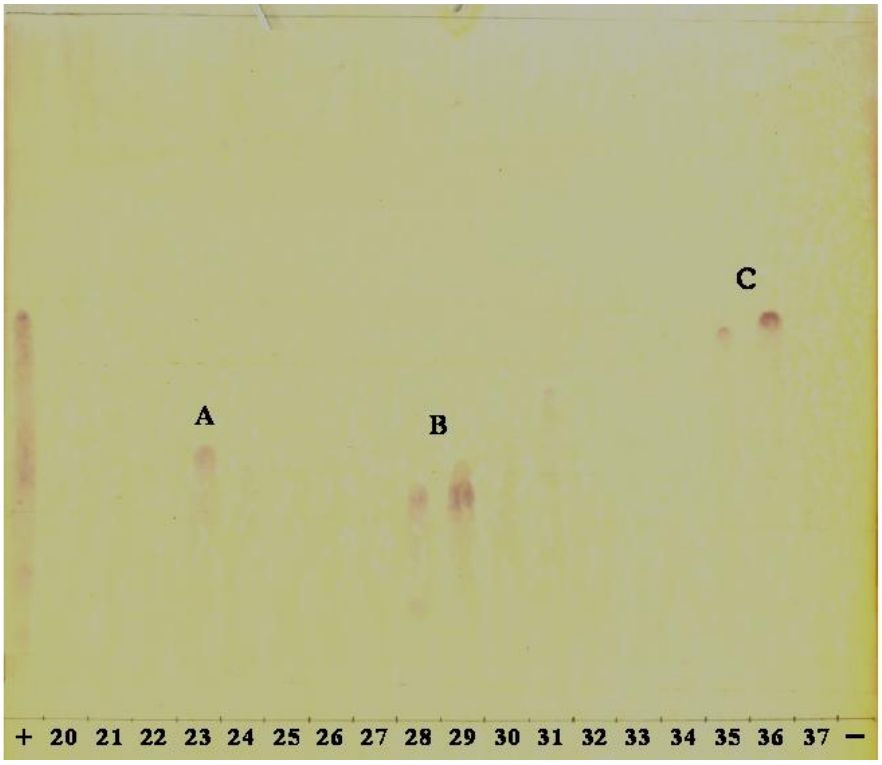

Figure 12: TLC plate showing three siderophore-like compounds revealed by HPLC of the LH-20 sample. Siderophore "A" is the least hydrophobic and "C" the most hydrophobic.

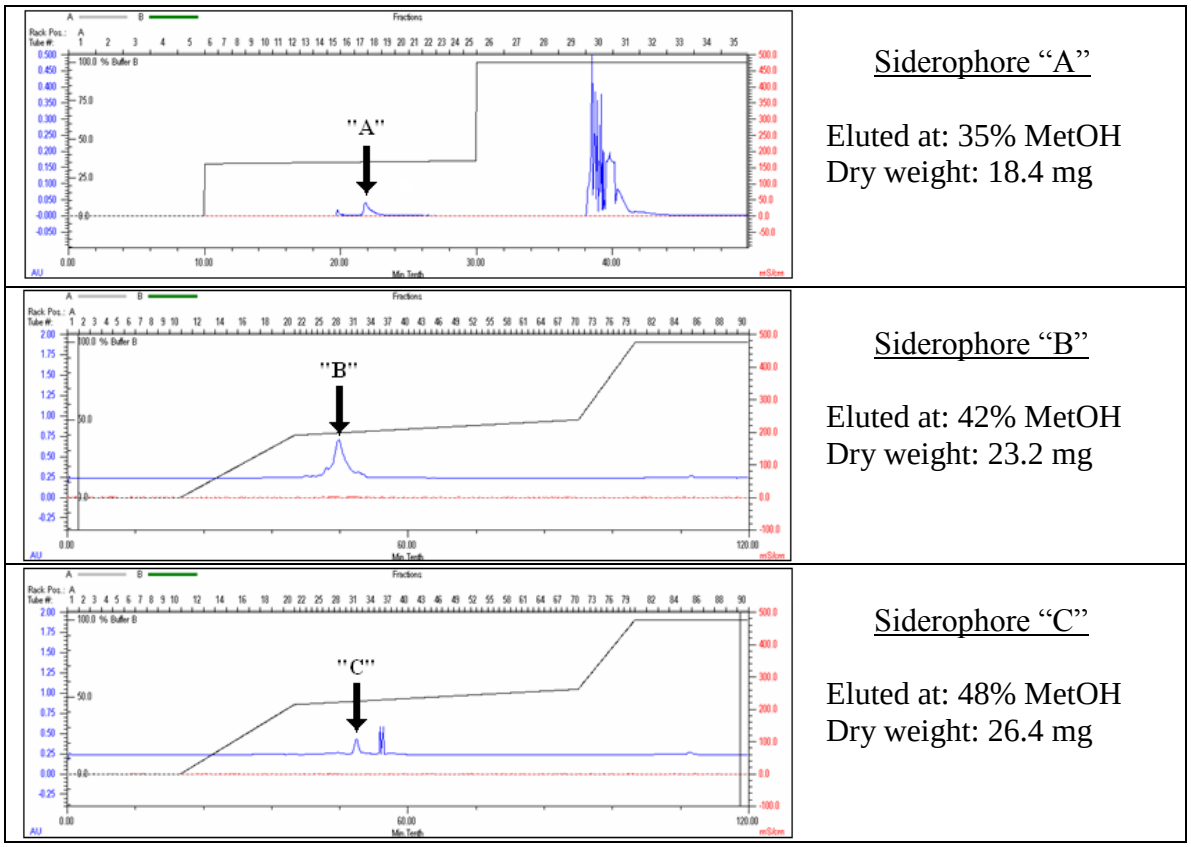

Figure 13: Final HPLC chromatograms generated for each of the three potential siderophores. Isolated peaks indicate that compound is pure.

Chemical Characterization of Purified Siderophores

Spectral Scan Analysis

Spectral absorbance analyses were used to determine the type of hydroxamate siderophore represented by each of the purified molecules. In general, maximum absorbance ranges of mono- and dihydroxamate siderophores are 500 – 520 nm, whereas trihydroxamate siderophores do so at 420 - 440 (Jalal and van der Helm 1991). All three absorbance maxima occur between the generally accepted ranges for hydroxamates (Figure 14). However, the maxima for both siderophores "B" and "C" (465 nm and 450 nm respectively) fall nearer to the trihydroxamate range, whereas the absorbance maximum for siderophore "A" (475 nm) is closer to that of dihydroxamates.

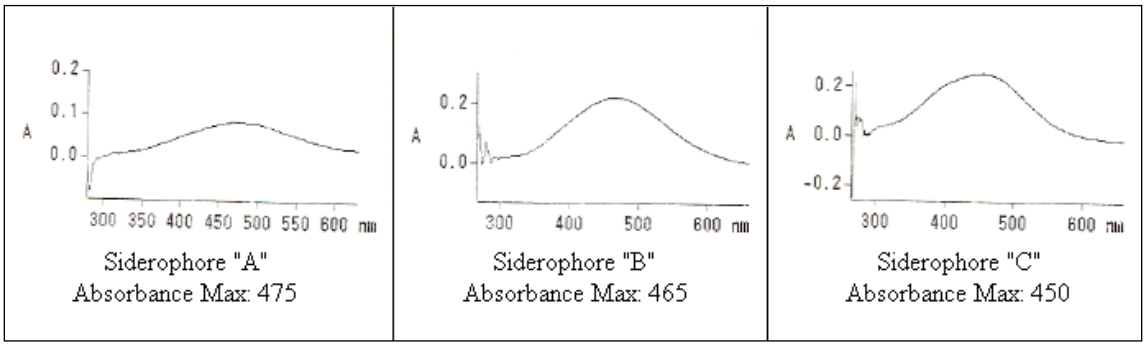

Figure 14: Spectral scans (300 – 600 nm) results of siderophores "A" (left), "B" (middle), and "C" (right). Mono- and Di-hydroxamate class siderophores absorb maximally at 500 – 520 nm. Tri-hydroxamate class siderophores absorb maximally at 420 – 440 nm (Jalal and van der Helm 1991).

Electrospray Mass Spectroscopy

To further chemically characterize the siderophore produced by *R. leguminosarum* ATCC 14479, six different samples were subject to mass spectroscopy. These samples consisted of one each of compounds A, B, and C in a deferriated form as well as one each of compounds A, B, and C in a ferriated form. Analyses of both the ferric- and apo-molecules allowed for comparisons between the spectra generated for each of the two forms. The lack of iron in the non-ferriated forms causes a difference of 53 [Fe^{3+} - 3H] in their molecular weights as compared to the ferric-complexes. Additionally, samples were ionized in both positive ion (protons added) and negative ion (protons removed) modes.

Figure 15 shows the accurate mass spectra generated at 25 volts for Siderophore C using the iron-free sample. In negative ion mode, the major peak was seen at 773.4 m/z. In positive ion mode, the major peak was seen at 775.3 m/z. This indicates that iron-free siderophore C has a total molecular weight of 774 because the mass of a proton, 1, must be subtracted from the positive ion mode results and added to the results from the negative ion mode analysis. Figure 16 shows the results obtained from analysis of the

iron-bound siderophore C sample in positive ion mode. The peak observed at 828 m/z corresponds to the molecular weight of siderophore C plus that of iron minus the three displaced hydrogen atoms plus the hydrogen atom added in positive ion mode [774 + 56 – 3 + 1]. The major peak seen at 850 m/z is the ferric chelate plus a sodium atom adduct [Na – H] that can be a common occurrence in this type of analysis. Table 4 summarizes the calculated accurate mass results for all six submitted samples. The ES/MS spectra generated for compounds "A" and "B" can be seen in Appendix figures 29 - 34.

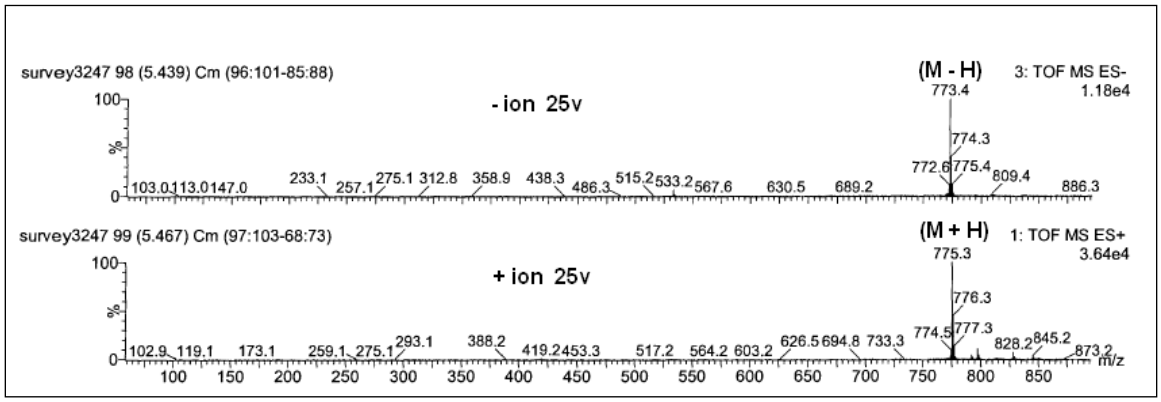

Figure 15: 25v ES/MS spectra for iron-free siderophore "C" in both negative (top) and positive ion (bottom) modes. The marked major peaks indicate the molecular weight of the compound +/- one proton.

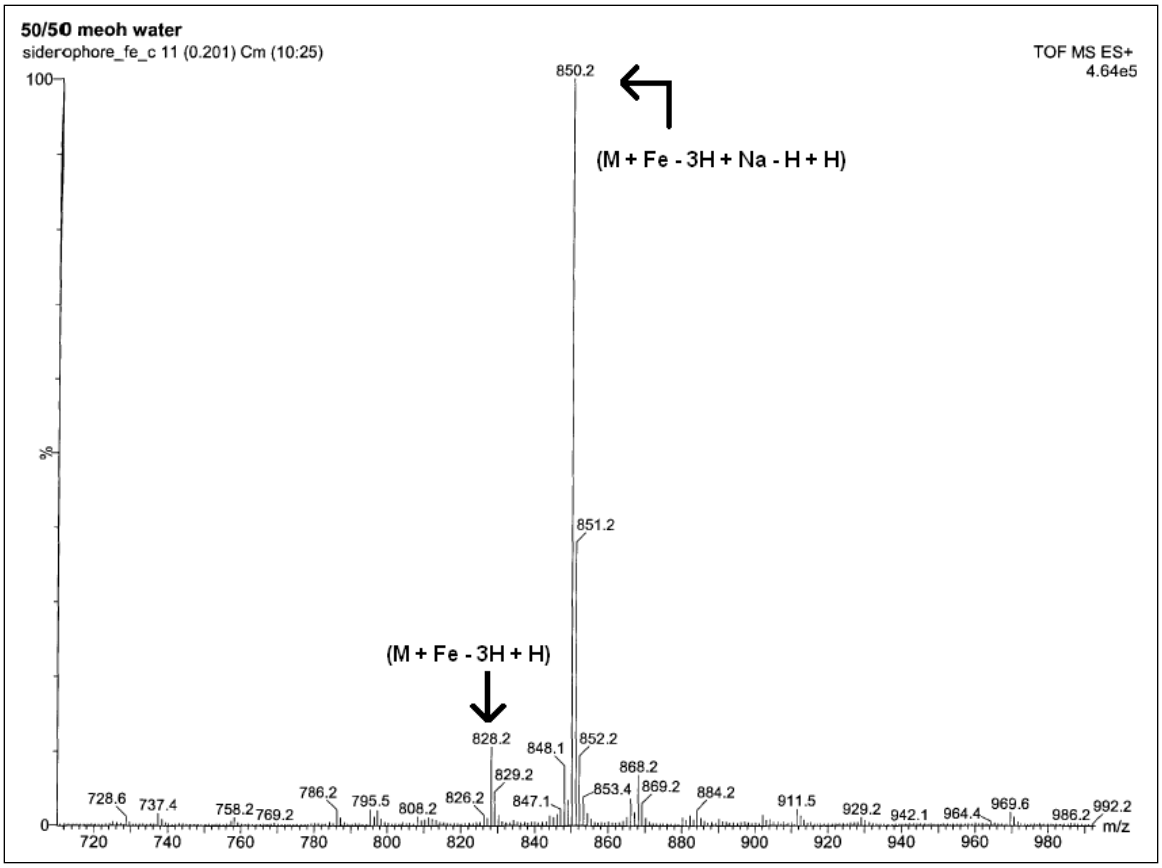

Figure 16: 25 v ES/MS spectra for iron-bound siderophore "C" in positive ion mode. The marked major peaks indicate the molecular weight of the ferric-compound both with and without a sodium (Na) adduct.

Table 4: Calculated molecular weights for siderophores "A", "B", and "C" in both ferriated and de-ferriated forms

Compound Sample	Calculated Molecular Weight	
	Iron-free	Iron-bound
A	492	545
B	750	803
C	774	828

In addition to determining the nominal molecular weight of the compounds, ES/MS was also used to determine molecular formulae from accurate mass determinations and substructural information from in-source collisionally induced dissociation (CID) spectra (Rozman et al. 1995). At higher cone voltages in the Waters electrospray source, molecular fragmentation is noted that can be used to determine substructural information for the compounds. Normally the nominal molecular weight is

determined at approximately 25 volts and substructural information is obtained in the range of 75 - 150 volts. The spectra at these higher voltages are noted in Figures 17 and 18.

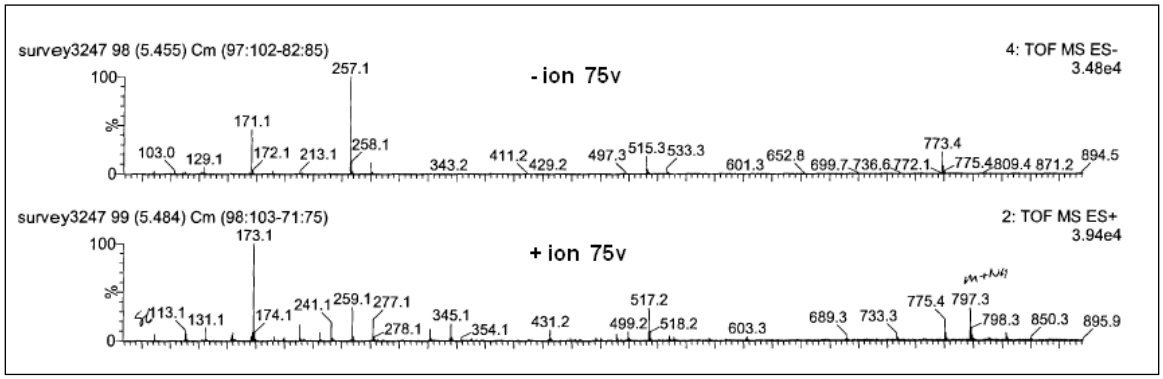

Figure 17: 75 v ES/MS fragmentation spectra for iron-free siderophore "C" in both negative (top) and positive ion (bottom) modes.

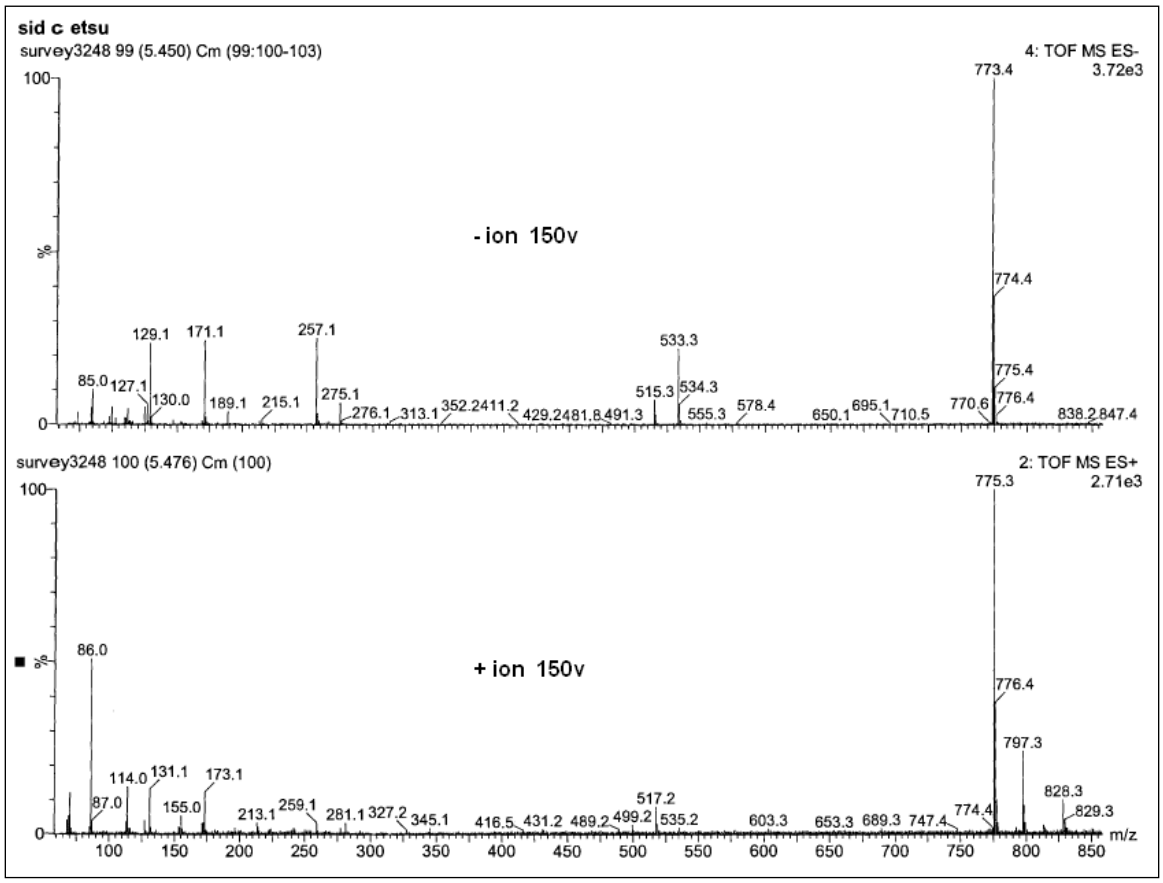

Figure 18: 150 v ES/MS fragmentation spectra for iron-free siderophore "C" in both negative (top) and positive ion (bottom) modes.

Using all the ES/MS data, an elemental composition report was generated. The molecular formula foe each compound was determined using the Waters Elemetnal Composition Program. The program limits the search by many user specified parameters including double bond equivalents, m/z error, odd or even electron species, and elements and their range. The error was estimated to be approximately 2 ppm (n=10, one standard deviation) (Figure 19). Normally the error specified for the search is at least three times the standard deviation. However, a window of 10 ppm was employed to insure that no reasonable candidate was excluded from the search. The elements searched and the ranges of their values were selected from known classes of siderophores. The theoretical isotopic pattern (generated using MassLynx Isotope Modeling Program) was visually compared to the observed pattern for further confirmation of structure. The boxed items in Figure 19 indicate the compositions whose theoretical isotope patterns best matched those seen produced by siderophores “A”, “B”, and “C” respectively (Appendix figures 35-36).

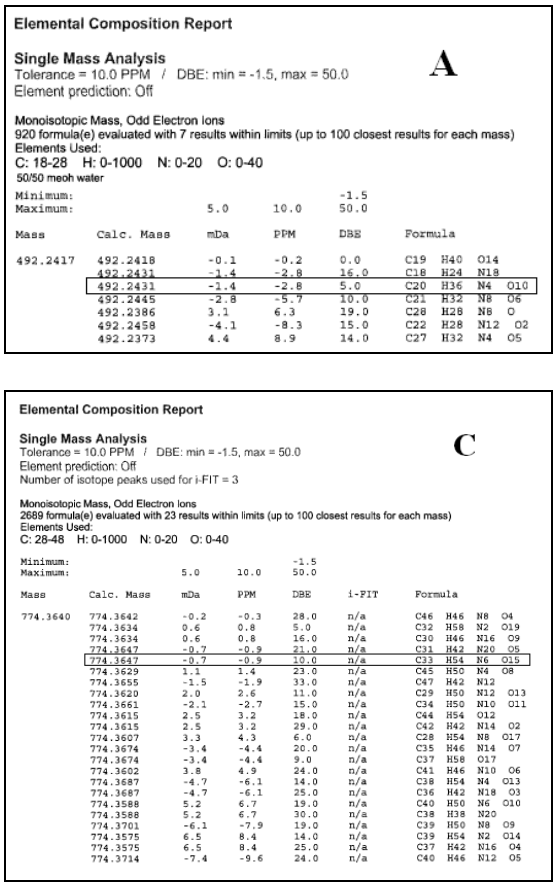

Elemental Composition Report

Single Mass Analysis **A**
Tolerance = 10.0 PPM / DBE: min = -1.5, max = 50.0
Element prediction: Off

Monoisotopic Mass, Odd Electron Ions
920 formula(e) evaluated with 7 results within limits (up to 100 closest results for each mass)
Elements Used:
C: 18-28 H: 0-1000 N: 0-20 O: 0-40
50/50 meoh water

Minimum:				-1.5	
Maximum:		5.0	10.0	50.0	
Mass	Calc. Mass	mDa	PPM	DBE	Formula
492.2417	492.2418	-0.1	-0.2	0.0	C19 H40 O14
	492.2431	-1.4	-2.8	16.0	C18 H24 N18
	492.2431	-1.4	-2.8	5.0	C20 H36 N4 O10
	492.2445	-2.8	-5.7	10.0	C21 H32 N8 O6
	492.2386	3.1	6.3	19.0	C28 H28 N8 O
	492.2458	-4.1	-8.3	15.0	C22 H28 N12 O2
	492.2373	4.4	8.9	14.0	C27 H32 N4 O5

Elemental Composition Report

Single Mass Analysis **C**
Tolerance = 10.0 PPM / DBE: min = -1.5, max = 50.0
Element prediction: Off
Number of isotope peaks used for i-FIT = 3

Monoisotopic Mass, Odd Electron Ions
2689 formula(e) evaluated with 23 results within limits (up to 100 closest results for each mass)
Elements Used:
C: 28-48 H: 0-1000 N: 0-20 O: 0-40

Minimum:				-1.5		
Maximum:		5.0	10.0	50.0		
Mass	Calc. Mass	mDa	PPM	DBE	i-FIT	Formula
774.3640	774.3642	-0.2	-0.3	28.0	n/a	C46 H46 N8 O4
	774.3634	0.6	0.8	5.0	n/a	C32 H58 N2 O19
	774.3634	0.6	0.8	16.0	n/a	C30 H46 N16 O9
	774.3647	-0.7	-0.9	21.0	n/a	C31 H42 N20 O5
	774.3647	-0.7	-0.9	10.0	n/a	C33 H54 N6 O15
	774.3629	1.1	1.4	23.0	n/a	C45 H50 N4 O8
	774.3655	-1.5	-1.9	33.0	n/a	C47 H42 N12
	774.3620	2.0	2.6	11.0	n/a	C29 H50 N12 O13
	774.3661	-2.1	-2.7	15.0	n/a	C34 H50 N10 O11
	774.3615	2.5	3.2	18.0	n/a	C44 H54 O12
	774.3615	2.5	3.2	29.0	n/a	C42 H42 N14 O2
	774.3607	3.3	4.3	6.0	n/a	C28 H54 N8 O17
	774.3674	-3.4	-4.4	20.0	n/a	C35 H46 N14 O7
	774.3674	-3.4	-4.4	9.0	n/a	C37 H58 O17
	774.3602	3.8	4.9	24.0	n/a	C41 H46 N10 O6
	774.3687	-4.7	-6.1	14.0	n/a	C38 H54 N4 O13
	774.3687	-4.7	-6.1	25.0	n/a	C36 H42 N18 O3
	774.3588	5.2	6.7	19.0	n/a	C40 H50 N6 O10
	774.3588	5.2	6.7	30.0	n/a	C38 H38 N20
	774.3701	-6.1	-7.9	19.0	n/a	C39 H50 N8 O9
	774.3575	6.5	8.4	14.0	n/a	C39 H54 N2 O14
	774.3575	6.5	8.4	25.0	n/a	C37 H42 N16 O4
	774.3714	-7.4	-9.6	24.0	n/a	C40 H46 N12 O5

Elemental Composition Report

Single Mass Analysis **B**
Tolerance = 10.0 PPM / DBE: min = -1.5, max = 50.0
Element prediction: Off
Number of isotope peaks used for i-FIT = 3

Monoisotopic Mass, Odd Electron Ions
2108 formula(e) evaluated with 19 results within limits (up to 100 closest results for each mass)
Elements Used:
C: 26-40 H: 0-1000 N: 0-20 O: 0-40
50/50 meoh water

Minimum:				-1.5		
Maximum:		5.0	10.0	50.0		
Mass	Calc. Mass	mDa	PPM	DBE	i-FIT	Formula
750.3643	750.3647	-0.4	-0.5	19.0	n/a	C29 H42 N20 O5
	750.3647	-0.4	-0.5	8.0	n/a	C31 H54 N6 O15
	750.3634	0.9	1.2	14.0	n/a	C28 H46 N16 O9
	750.3634	0.9	1.2	3.0	n/a	C30 H58 N2 O19
	750.3661	-1.8	-2.4	13.0	n/a	C32 H50 N10 O11
	750.3620	2.3	3.1	9.0	n/a	C27 H50 N12 O13
	750.3615	2.8	3.7	27.0	n/a	C40 H42 N14 O2
	750.3674	-3.1	-4.1	18.0	n/a	C33 H46 N14 O7
	750.3674	-3.1	-4.1	7.0	n/a	C35 H58 O17
	750.3607	3.6	4.8	4.0	n/a	C26 H54 N8 O17
	750.3602	4.1	5.5	22.0	n/a	C39 H46 N10 O6
	750.3687	-4.4	-5.9	12.0	n/a	C36 H54 N4 O13
	750.3687	-4.4	-5.9	23.0	n/a	C34 H42 N18 O3
	750.3588	5.5	7.3	28.0	n/a	C36 H38 N20
	750.3588	5.5	7.3	17.0	n/a	C38 H50 N6 O10
	750.3701	-5.8	-7.7	17.0	n/a	C37 H50 N8 O9
	750.3575	6.8	9.1	12.0	n/a	C37 H54 N2 O14
	750.3575	6.8	9.1	23.0	n/a	C35 H42 N16 O4
	750.3714	-7.1	-9.5	22.0	n/a	C38 H46 N12 O5

Figure 19: Elemental composition report indicating possible chemical formulae for "A", "B", and "C". Results are based on the accurate mass and fragmentation data obtained from mass spectroscopy. The boxed items are consistent for the trihydroxamate siderophore vicibactin (C) and two degradation products (A and B)

These results, along with the fragmentation data, also allowed structures to be proposed for each of the siderophore samples analyzed. Figure 20 shows these proposed structures. The molecular weight and composition results for siderophore "C" were both consistent for vicibactin ($C_{33}H_{55}N_6O_{15}$), a trihydroxamate siderophore commonly produced by *R. leguminosarum* bv. *viciae*. This is also supported by our spectral scan analysis which showed siderophore "C" to maximally absorb light at 450 nm. Dilworth, et al. (1998) found the vicibactin absorbance maximum to be 445 nm. Due to the similarity in fragmentation results for all three compounds, it was concluded that they each shared a similar structure. For this reason, it was decided that siderophores "A" and "B" were likely degradation products of "C" as the purification process can often times lead to the breakdown of a molecule. Each of these products appears to be a de-

acetylated and “ring-open” structure in which the cyclic nature of the vicibactin has been compromised. In siderophore “B”, a single ester-bond linkage has been hydrolyzed. In siderophore “A”, two ester-bonds have been hydrolyzed resulting in the loss of approximately one-third of the intact siderophore.

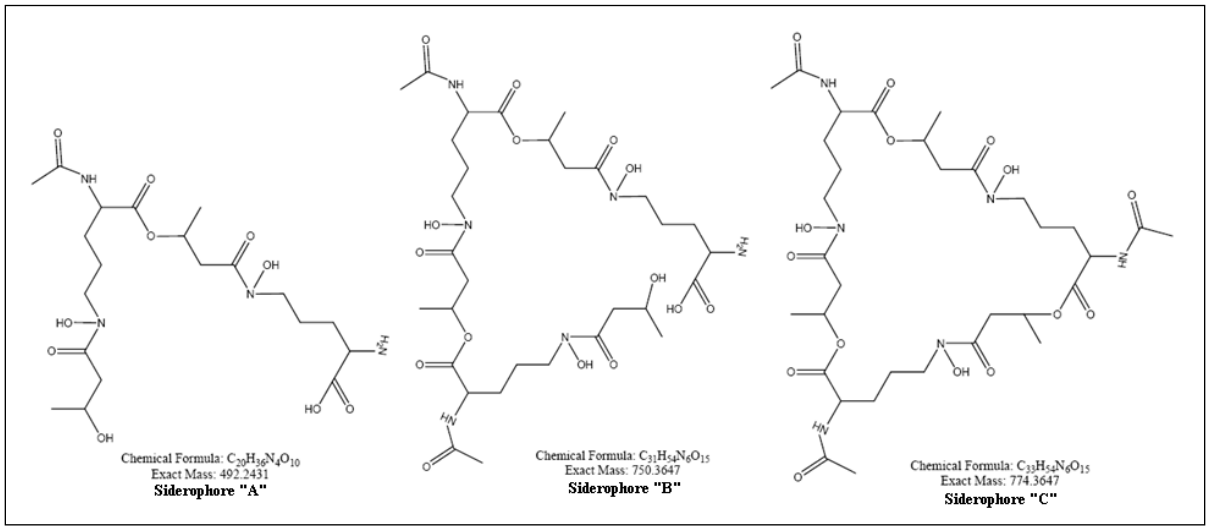

Figure 20: Proposed structures for siderophores “A”, “B”, and “C”. The formula and structure of siderophore “C” match that of the trihydroxamate siderophore, vicibactin.

Nuclear Magnetic Resonance (NMR) Spectroscopy

NMR was used to confirm the molecular structures proposed by the ES/MS data. The proton NMR resonances for each of the three compounds were compared to the known data for vicibactin (Dilworth et al. 1998). The chemical shifts and multiplicities for siderophore “C” correspond extremely well with those shown in the literature (Table 5). The NMR spectra for “A” and “B” (Figures 23 and 22 respectively) are both similar to that of “C” (Figure 21). This indicates that they each share very similar structures to that of vicibactin consistent with our proposed structures.

Table 5: Proton NMR data for siderophore "C" and vicibactin. Literature values and position assignments taken from Dilworth et al. 1998. (Multiplicity values: s = singlet; d = doublet; dd = doublet of doublets; m = multiplet)

Carbon Position	Bond Type	Literature Values for Vicibactin		Experimental Values for compound "C"	
		^{1}H, PPM	Multiplicity	^{1}H, PPM	Multiplicity
2	α-CH	4.29	dd	4.3	dd
3	β-CH_2	1.60	m	1.6	m
		1.79	m	1.8	m
4	γ-CH_2	1.68	m	1.7	m
5	δ-CH_2	3.55	m	3.5	m
		3.64	m	3.6	m
7	α-CH_2	2.69	dd	2.7	dd
		2.86	dd	2.8	dd
8	β-CH	5.38	m	5.4	m
9	γ-CH_3	1.32	d	1.3	d
12	CH_3	1.99	s	2.0	s

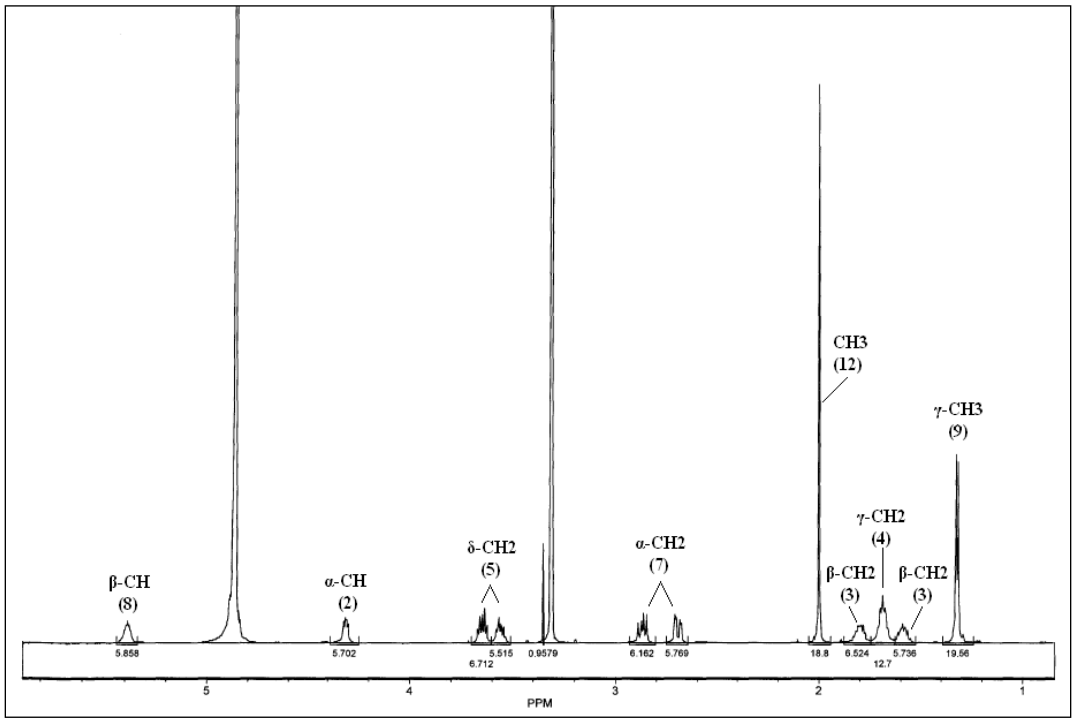

Figure 21: Proton NMR spectrum for purified siderophore "C". Numbers in parentheses correspond to the numbering assignments for carbon atoms as given in Dilworth et al. 1998.

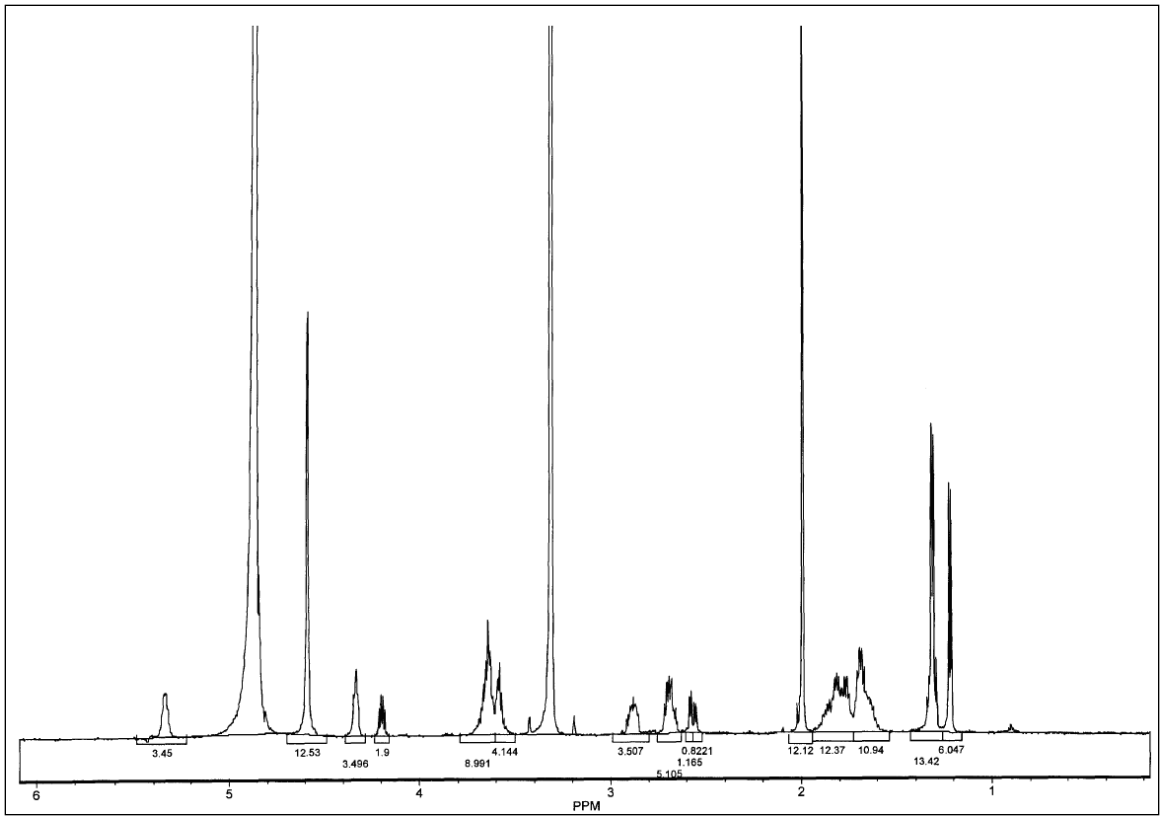

Figure 22: Proton NMR spectrum for purified siderophore "B".

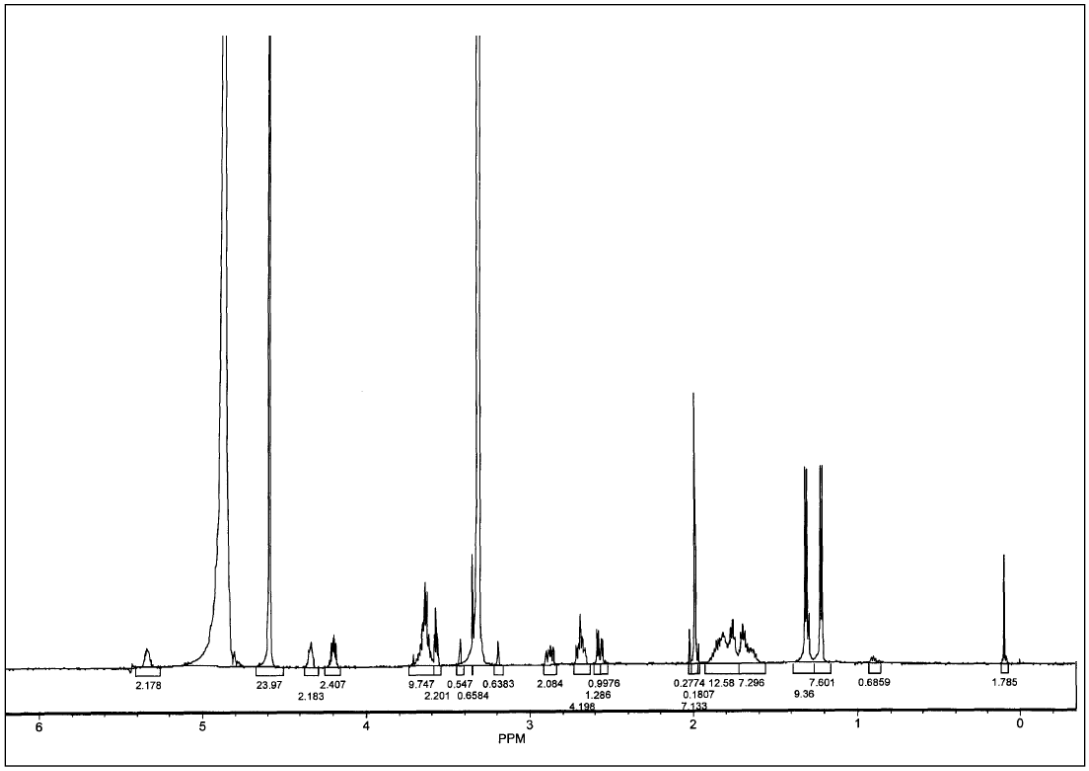

Figure 23: Proton NMR spectrum for purified siderophore "A"

Deuterium Exchange Analysis

Deuterium exchange was conducted on each of the pure iron-free samples to determine if the proposed ring-open structures were feasible. Samples were dissolved in a 50:50 acetonitrile-d3:deuterium oxide solution and analyzed via mass spectroscopy in both positive and negative ionization modes. This allowed a count of the number of exchangeable protons (any hydrogen atoms bound to either O or N). Deuterium, or "heavy hydrogen", is composed of a hydrogen atom plus one neutron bringing its total mass to roughly 2 amu. Deuterium increases the mass of a given molecule by 1u for each instance that it is exchanged with hydrogen. Figures 24 - 26 show the chromatograms generated for each of the samples. The product for "C" showed six exchangeable protons in both positive and negative modes. Siderophores "A" and "B" have seven and nine exchangeable protons respectively. This is consistent with both of the proposed ring-opened and de-acetylated compound structures. These results are summarized in Table 6.

Table 6: Deuterium exchange results showing the number of exchangeable hydrogen atoms bound to either an oxygen or nitrogen atom.

Compound	MW	Calculated MW after Deuterium Exchange	# Exchangeable Protons
A	492	499	7
B	750	759	9
C	774	780	6

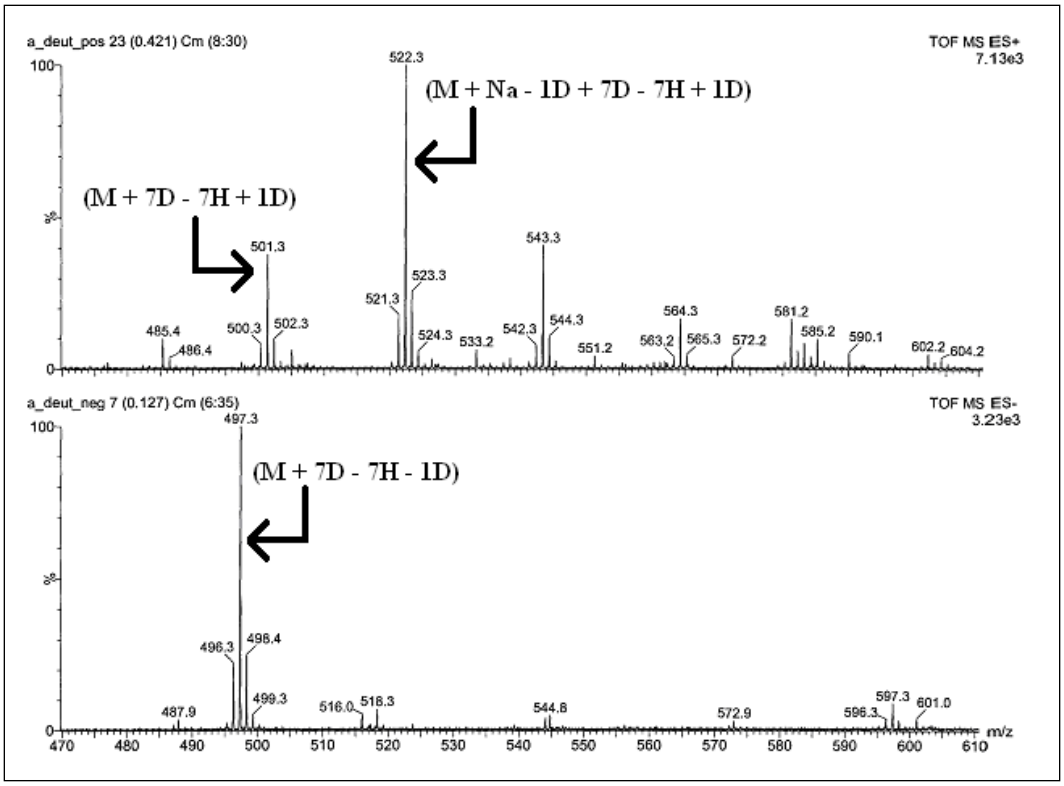

Figure 24: Deuterium exchange results for siderophore "A" in both positive ion (top) and negative ion (bottom) modes.

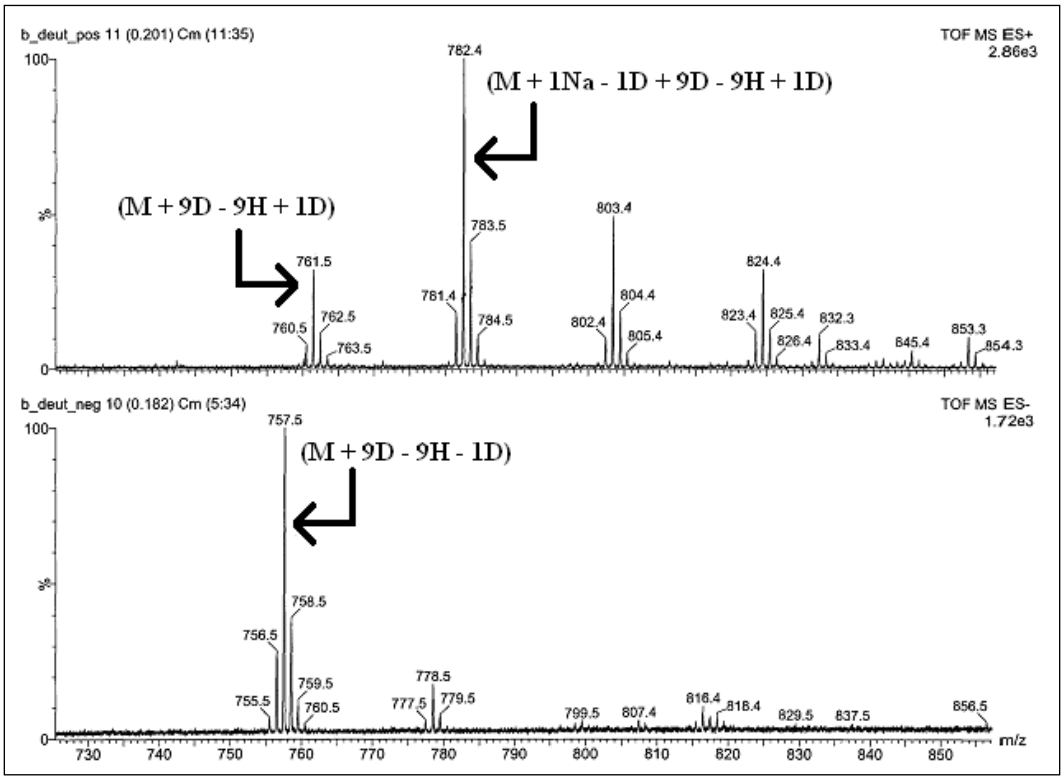

Figure 25: Deuterium exchange results for siderophore "B" in both positive ion (top) and negative ion (bottom) modes.

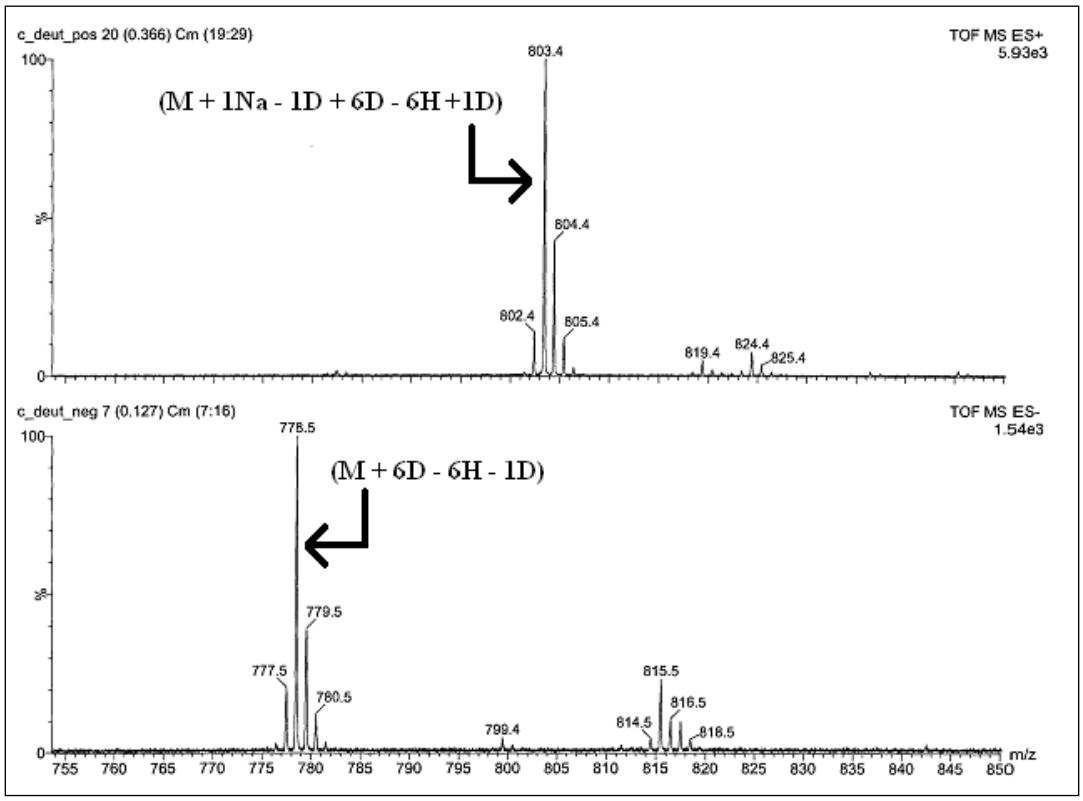

Figure 26: Deuterium exchange results for siderophore “C” in both positive ion (top) and negative ion (bottom) modes.

Amino Acid Analysis Using TLC

To further characterize the proposed structures and identify the molecules, acid hydrolyzed samples of each compound were analyzed for their amino acid content. These samples were run on a TLC plate and developed with a ninhydrin reagent. These were compared against an ornithine standard because vicibactin is composed of three residues each of hydroxybutanoic acid and the amino acid ornithine (Dilworth et al. 1998). All three samples showed only a single, strong spot at an Rf value of 0.78, very near the Rf value, 0.74, of pure ornithine (Figure 27). The formation and Rf value of the single spot for each compound indicated that all three purified molecules contained only ornithine residues as an amino acid.

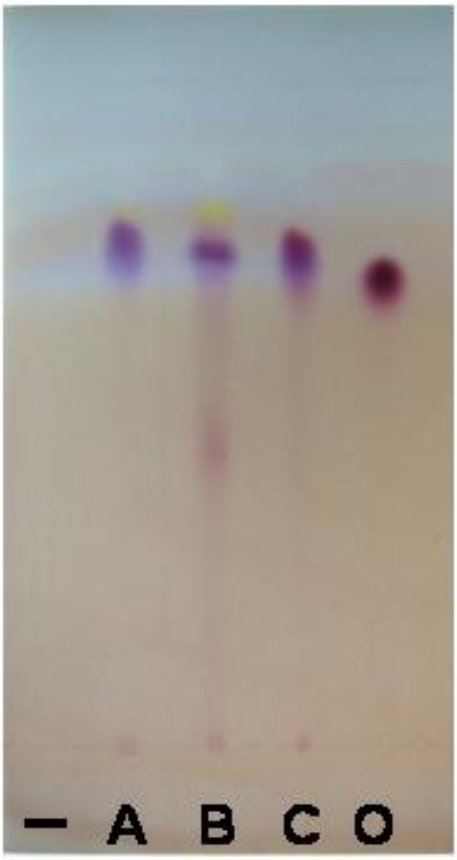

Figure 27: Amino acid analysis using TLC shows that each hydrolyzed sample contained only the amino acid ornithine (O).

CHAPTER 4

DISCUSSION

Iron is a requirement for the synthesis of many bacterial compounds and is an essential nutrient for growth. Many bacteria, both gram-negative and gram-positive, have been found to produce siderophores in response to iron deprivation. Siderophore production is particularly abundant within the rhizobial group of bacteria. Most species within this group have been found to produce at least one type of siderophore with rhizobactin (Smith et al. 1985), rhizobactin 1021 (Persmark et al. 1993), and vicibactin (Dilworth et al. 1998) being the most common.

Rhizobial microorganisms are of economic and social interest due to their agricultural importance. The symbiosis between the bacteria and its host plant is exhibited by the formation of root nodules. Within the nodules the bacteria fix atmospheric nitrogen into biologically useful compounds that are shared with the host. Proper formation of these nodules is dependent upon sufficient iron acquisition by the bacteria (O'Hara et al. 1988). Additionally, due to the competition for iron, siderophore production has been identified as one an important mechanism for the suppression of phytopathogens (Arora et al. 2001).

The objective of this project was to determine whether *Rhizobium leguminosarum* ATCC 14479 produced a siderophore and, if so, to characterize and identify siderophores from this previously uncharacterized strain. The CAS assay showed evidence that this strain did produce a siderophore while under iron-deprived conditions. The presumed siderophore was determined to be in the hydroxamate family of siderophores as

evidenced by the formation of a wine red color using the iron-perchloate assay (Atkin et al. 1970).

Growth conditions were then optimized to achieve maximum siderophore production. Initially, optimized conditions included only media composition and incubation time. The defined minimal media of Manhart and Wong (1979) was modified and used to grow this strain. Although it is known that members of the rhizobia group prefer mannitol (Murray and Smith, 1957), both mannitol and arabinose were replaced with dextrose as the carbon source. Also, glutamate was used in place of KNO_3 as a nitrogen source (Streeter 1985). Many rhizobia are known to grow relatively slowly as compared to other bacteria and it was found that an incubation time of 96 hours was necessary to reach maximum siderophore production. Like many secondary metabolites, onset of siderophore production normally occurs in the mid-log phase of growth. *R. leguminosarum* ATCC 14479 begins producing siderophore approximately 36 hours after inoculation and reaches siderophore production peak at 96 to 100 hours.

For the isolation of siderophore, culture growth was carried out in a zero iron concentration media. Following characterization of siderophore, iron concentration was optimized because production of these molecules is regulated by iron availablity (Lankford 1973). As seen in other rhizobia, *R. leguminosarum* ATCC 14479 demonstrated a biphasic relationship of iron concentration on siderophore production. When iron was completely removed from the media, no siderophore was produced. Siderophore production improved when supplemented with low levels of iron but decreased and was eventually completely repressed as the iron concentration increased. It was found that this strain produces maximally when the media is supplemented with 0.25 μM $FeCl_3$. Our data indicated that this concentration of iron supplement resulted in

a doubling of siderophore production. Siderophore production then decreased as this concentration is exceeded until being completely repressed at 1.0 μM. This is in good accord with the findings of Carson et al. (2000) in which they found that siderophore production was repressed in other rhizobia within a range of 1-5 μM concentration.

Large batch cultures of *Rhizobium leguminosarum* ATCC 14479 were grown in order to produce sufficient quantities of siderophore to isolate and characterize. Initial purification involved passing acidified culture supernatant through a XAD-2 column. Siderophore positive elutions from the XAD column were then concentrated and passed through a Sephadex LH-20 hydrophobic column. Final purification of our compounds was conducted using HPLC with a C_{18} hydrophobic column.

Multiple spots appeared on the TLC plates when purified sample was loaded onto them. This occurred once following elution of the LH-20 column and then again following the initial HPLC trials, creating a total of three distinct TLC spots. Although multiple spot formations could indicate the presence of multiple siderophores, it is also possible for siderophores to degrade during the purification process but still retain their ability to chelate ferric iron. Therefore, the compounds represented by these spots were purified separately and labeled as siderophores "A", "B", and "C" in order of increasing hydrophobicity. Spectral scans (300 - 700 nm) were conducted on each of these molecules to determine whether they were mono/di- or tri-hydroxamate type siderophores (Jalal and van der Helm 1991). Absorbance results were somewhat inconclusive as all three molecules had different absorbance maxima that fell outside of the expected ranges. However, it was our belief that siderophore "C" was most likely a tri-hydroxamate as its

absorbance maximum did fall very near the expected upper range of that group of siderophores.

Electrospray Mass Spectroscopy (ES/MS) was performed on all three of the purified compounds to elucidate their molecular weights and structures. Based on the results of this analysis it was proposed that "C" was the trihydroxamate siderophore, vicibactin. It also indicated that "A" and "B" were degradation products of the intact siderophore. This was then confirmed by NMR, deuterium exchange, and amino acid analysis. Whether these degradation products are a result of the purification process or if they are produced inside the cell and released into the culture medium is unknown.

Vicibactin is a cyclic trihydroxamate siderophore made up of three residues each of D-3-hydroxybutyric acid and N^2-acetyl-N^5-hydroxy-D-ornithine bonded by alternating amide and ester bonds (Dilworth et al. 1998). Originally discovered being excreted by *Rhizobium leguminosarum* biovar *viciae,* which nodulates peas, lentils, and vetches, it has since been implicated to be the siderophore most often produced by all siderophore positive strains of *Rhizobium leguminosarum* (Carson et al. 1994; 2000). Its structure is very similar to other bacterial (desferrioxamines) and fungal (fusarinines) trihydroxamate siderophores (Figure 28). In fact, bacterial vicibactin is structurally identical to fungal neurosporin, isolated from *Neurospora crassa* (Eng-Wilmot et al. 1983), although the biosynthesis strategies appear to have evolved separately (Heemstra et al. 2009).

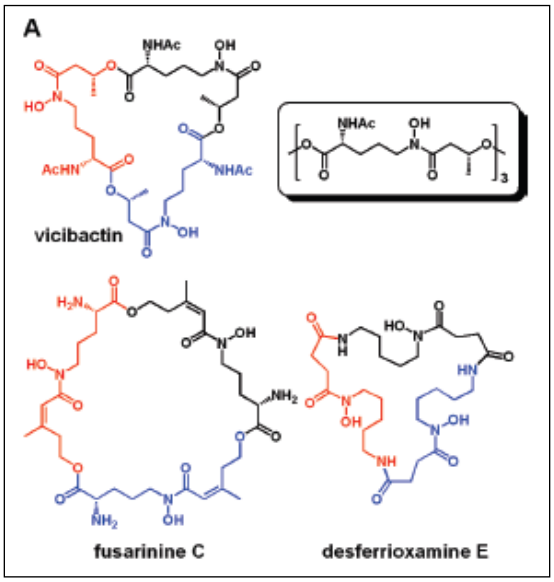

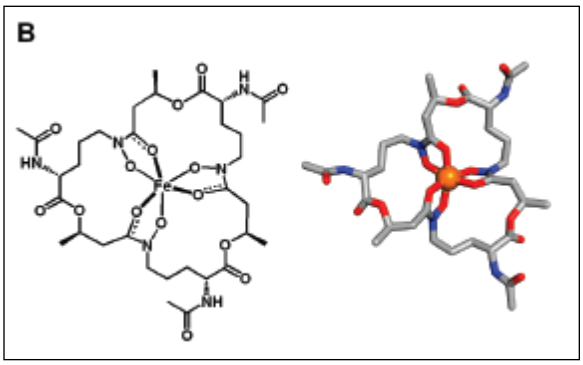

Figure 28: (A) Similar trimeric hydroxamate siderophores from bacteria (vicibactin and desferrioxamine E) and fungi (fusarinine C). (B) Structure of ferric-vicibactin chelate. This structure is identical to that of ferric-neurosporin. (Heemstra et al. 2009)

Biosynthesis of vicibactin in *Rhizobium leguminosarum* biovar *viciae* was found to be controlled by a cluster of eight genes, *vbsGSO*, *vbsADL*, *vbsC*, and *vbsP* (Carter et al. 2002). They proposed a metabolic biosynthesis pathway citing the gene product of *vbsS* as the single NRPS (non-ribosomal peptide synthase) module protein acting as the primary siderophore catalyst. NRPSs are multi-part enzymes, similar to an assembly line, that produce sequence specific peptide products without an RNA template. Instead, the order of specialized NRPS domains dictates the order that the monomeric amino acids are linked (Crosa and Walsh 2002). Uptake of the ferric-vicibactin chelate has been identified to be mediated by homologues of the *E. coli fhu* operon, *fhuACDB*. In *E.coli*, FhuA is the outer-membrane receptor protein, FhuB is a cytoplasmic membrane protein, FhuC is an ATPase, and FhuD is the periplasmic transport protein (Stevens et al. 1999). In *R. leguminosarum* bv. *viciae*, *fhuCDB* are in one operon adjacent to an inactive *fhuA* pseudogene containing many stop codons (Stevens et al. 1999). Yeoman et al. (2000)

located a fully functional unlinked *fhuA* gene that is unlinked to the rhizobial *fhuCDB* operon. Mutations in this version of *fhuA* resulted in impaired iron uptake and large CAS halo phenotypes, indicating overproduction of siderophore due to an inability to internalize the ferric-vicibactin.

To date, only one study (Carson *et al*, 2000) has linked vicibactin production with clover infecting strains of *R. leguminosarum*. Further research for this project includes identification and comparison of *R. leguminosarum* ATCC 14479 vicibactin biosynthesis and transport mechanisms with those of other *Rhizobium* species. Due to its identical structure, it would also be of interest to compare these mechanisms to those of *Neurospora*'s siderophore, neurosporin.

REFERENCES

Arora, N. K., Kang, S. C., and Maheshwari, D. K. 2001. Isolation of siderophore-producing strains of Rhizobium meliloti and their biocontrol potential against Macrophomina phaseolina that causes charcoal rot of groundnut. Current Science. 81 (6): 673 – 677.

Arnow, L. E. 1937. Colorimetric determination of the components of 3,4-dihydroxyphenylalanine-tyrosine mixtures. J. Biol. Chem. 118:531-537.

Atkin, C. L., J. B. Neilands, and H. J. Phaff. 1970. Rhodotorulic acid from species of Leucosporidium, Rhodosporidium, Rhodotorula, Sporidiobolus, and Sporobolomyces, and a new alanine-containing ferrichrome from Cryptococcus melibiosum. J. Bacteriol. 103: 722-733.

Bergerson, F. J. 1961. The growth of Rhizobium in synthetic media. Aust. J. Biol. Sci. 14: 349.

Boyer, R. Modern Experimental Biochemistry. 3rd ed. San Francico: Addison Wesley Longman, 2000.

Carson, K. C., Glenn, A. R., and Dilworth, M. J. 1994. Specificity of siderophore-mediated transport of iron in rhizobia. Arch Microbiol 161: 333–339.

Carson, K. C., J. Meyer, and M. J. Dilworth. 2000. Hydroxamate siderophores of root nodule bacteria. Soil Biol. and Biochem. 32:11-21.

Carter, R. A., Worsley, P.S., Sawers, G., Challis, G. L., Dilworth, M. J., Carson, K. C., Lawrence, J. A., Wexler, M., Johnston, A. W., and Yeoman, K. H. 2002. The *vbs* genes that direct synthesis of the siderophore vicibactin in *Rhizobium leguminosarum*: their expression in other genera requires ECF σ factor Rpol. Molecular Microbiology. 44(5): 1153 – 1166.

Chakraborty, R., E. Lemke, Z. Cao, P. E. Klebba, and D. van der Helm. 2003. Identification and mutational studies of conserved amino acids in the outer membrane receptor protein, FepA, which affect transport but not binding of ferric-enterobactin in Escherichia coli. Biometals. 16: 507 - 518.

Chi, et al. 2007. Periplasmic Proteins of the extremophile *Acidithiobacillus ferrooxidans.* Molecular and Cellular Proteomics. 6: 2239 - 225.

Clement, E., Mesini, P., Pattus, F., and Schalk, I. 2004. The binding mechanism of pyoverdin with the outer membrane receptor FpvA in Pseudomonas aeruginosa is dependent on its iron-loaded status. Biochemistry. 43(24): 7954 - 7965.

Crosa, J., Alexandra, M., and Shelley Payne. Iron Transport in Bacteria. Washington D.C.: ASM Press, 2004.

Crosa, J. H. and C. T. Walsh. 2002. Genetics and assembly line enzymology of siderophore biosynthesis in bacteria. Microbiol. Mol. Biol. Rev. 66: 223 - 249.

Das, Asparajita, et al. 2007. Fungal Siderophores: Structures, Function and Regulation. In Ajit Varma and S. B. Chincholkar (Eds.), *Soil Biology v. 12: Microbial Siderophores* (1st ed., pp. 1-42). Berlin Heidelberg, Germany: Springer.

Dave, B., et al. 2006. Siderophores of halophilic archaea and their chemical characterization. Ind. J. Exp. Bio. 44: 340 - 344.

Dilworth, M. J., K. C. Carson, R. G. F. Giles, L. T. Byrne, and A. R. Glenn. 1998. Rhizobium leguminosarum bv. viciae produces a novel cyclic trihydroxamate siderophore, vicibactin. Microbiol. 144: 781 - 791.

Drechsel, H. and G. Jung. 1988. Peptide Siderophores. J. Peptide Science. 4: 147 - 181.

Drechsel, H., Tschierske, M., Thieken, A., Jung, G., Zahner, H., and Winklemann, G. 1995. The carboxylate type siderophore rhizoferrin and its analogs produed by directed fermentation. Journal of Industrial Microbiolgy. 14: 105 - 112.

Egli, Thomas. 2003. Nutrition of Microorganisms. In Moselio Schaechter (Ed.), *The Desk Encyclopedia of Microbiology* (1st ed., pp. 725-738). San Diego, Ca: Elsevier Ltd.

Eng-Wilmot, D. L., Rahman, A., Mendenhall, J. V., Grayson, S. L., and van der Helm, D. 1984. Molecular Structure of Ferric Neurospoin, a minor siderophore-like compound containing N-Hydroxy-D-ornithine. J. Am. Chem. Soc. 106: 1285 – 1290.

Falkowski, P. G. 1997. Photosynthesis: the paradox of carbon dioxide efflux. Curr. Biol. 7: R637 - R639.

Fischbach, M. A., and Walsh, C. T. 2006. Assembly-line enzymology for polyketide and nonribosomal Peptide antibiotics: logic, machinery, and mechanisms. Chem Rev. 106: 3468 - 96.

Guerinot, Mary L. 1994. "Microbial Iron Transport". Annual Review of Microbiology. 48: 743 - 72.

Guerinot, M. L., E. J. Meidl, and O. Plessner. 1990. Citrate as a siderophore in Bradyrhizobium japonicum. J. Bacteriol. 172: 3298 - 3303.

Hammond, David. 2008. Characterization of the Genes Involved in Biosynthesis and Transport of Schizokinen, a Siderophore produced by *Rhizobium leguminosarum* IARI 917. M. S. Thesis. East Tennessee State University, Johnson City, TN.

Hamza, I., S. Chauhan, R. Hassett, and M. R. O'Brian. 1998. The bacterial Irr protein is required for coordination of heme biosynthesis with iron availability. J. Biol. Chem. 273: 21669 - 21674.

Heemstra, J., Walsh, C., and Sattely, E. 2009. Enzymatic Tailoring of Ornithine in the Biosynthesis of the *Rhizobium* Cyclic Trihydroxamate Siderophore Vicibactin. J. Am. Chem. Soc. 131: 15317 – 15329.

Hemling, M., Conboy, J., Bean, M., Mentzer, M., and Carr, S. 1994. Gas phase hydrogen –deuterium exchange in electrospray ionization mass spectrometry as a practical tool for structure elucidation. Journal of the American Society for Mass Spectrometry. 5(5): 434 – 442.

Hunt, M. D., Pettis, G. S., and McIntosh, M. A. 1994. Promoter and operator determinants for fur-mediated iron regulation in the bidirectional *fepA-fes* control region of the *Escherichia coli* enterobactin gene system. J Bacteriol 176: 3944 - 55.

Jadhav, R. S., and Desai A. J. 1996. Effect of nutritional and environmental conditions on siderophore production by *Rhizobium GN1* (peanut isolate). Ind. J. Expt. Biol. 34: 436 - 439.

Jalal, M. A. F., and D. van der Helm. 1991. Isolation and spectroscopic identification of fungal siderophores. p. 235-269. In G. Winkelmann (ed.), CRC handbook of microbial iron chelates. CRC Press, Boca Raton, Fl.

Johnston, A. W. B. 2004. Mechanisms and regulation of iron upatke in the Rhizobia, p. 469-488. In J. H. Crosa, A. R. Mey, and S. M. Payne (ed.), Iron Transport in Bacteria. ASM Press, Washington, D.C.

Kim, M., Fanucci, G., and Cafiso, D. 2007. Substrate-dependent transmembrane signaling in TonB-dependent transporters is not conserved. PNAS. 104(29): 11975 - 11980.

Kneen, B. E. and LaRue, T. A. 1983. Congo red absorption by *Rhizobium leguminosarum*. Appl. Environ. Microbiol. 45: 340-342.

Lam, W. and Ragu Ramanathan. 2002 . In electrospray ionization source hydrogen/deuterium exchange LC-MS and LC-MS/MS for characterization for characterization of metabolites. Journal of the American Society for Mass Spectrometry. 13(4): 345 – 353.

Lankford, C. E. 1973. Bacterial assimilation of iron. Crit. Rev. Microbiol. 2: 273 - 331.

Loh, J., and G. Stacey. 2003. Nodulation gene regulation in Bradyrhizobium japonicum: a unique integration of global regulatory circuits. Appl. Environ. Microbiol. 69: 10 - 17.

Loprasert, S., Sallabhan, R., Atichartpngkul, S., and Mongkolsuk, S. 1999. Characterization of a ferric uptake regulator (fur) gene from Xanthomonas campestris pv. Phaseoli with unusual primary structure, genome organization, and expression patterns. Gene. 239: 251 - 258.

Manhart, James and Peter Wong. 1979. Nitrate reductase activities of rhizobia and the correlation between nitrate reduction and nitrogen fixation. Can. J. Microbiol. 25(10): 1169 – 1174.

Meneely, K. 2007. The biochemistry of siderophore biosynthesis. Diss. University of Kansas, Lawrence, KS.

Miethke, M. and Marahiel, M. 2007. Siderophore-Based Iron Acquisition and Pathogen Control. Microbiology and Moleculuar Biology Reviews. 71(3): 413 - 451.

Murray, E. G. D., and N. R. Smith. 1957. Bergey's Manual of Determinative Biology, 7th edition. The William's and Wilkin's Company, Maryland.

Nadler, K. D., A. W. B. Johnston, J. Chen, and T. R. John. 1990. A *Rhizobium leguminosarum* mutant defective in symbiotic iron acquisition. J. Bacteriol. 172: 670 - 677.

Neilands, J. B. 1984. Methodology of Siderophores, Structure and Bonding. 58: 1 - 24.

O' Brien, I. G., and F. Gibson. 1970. The structure of enterochelin and related 2,3-dihydroxy-N-benzoyl-serine conjugates from *Escherichia coli*. Biochim. Biophys. Acta 215: 393 - 402.

O'Hara GW, Dilworth MJ, Boonkerd N, Parkpian P. 1988. Iron deficiency specifically limits nodule development in peanut inoculated with *Bradyrhizobium* sp. New

Phytol 108: 51 - 57.

Patel, H. M., and Walsh, C. T. 2001. In vitro reconstitution of the *Pseudomonas aeruginosa* nonribosomal peptide synthesis of pyochelin: characterization of backbone tailoring thiazoline reductase and N-methyltransferase activities. Biochemistry 40: 9023 - 31.

Pawelek P, Croteau N, Ng-Thow-Hing C, Khursigara C, Moiseeva N, Allaire M, Coulton JW. 2006. Structure of TonB in complex with FhuA, E. coli outer membrane receptor. Science. 312 (5778): 1399 - 1402.

Persmark, M., P. Pittman, J. S. Buyer, B. Schwyn, P. R. Gill, Jr., and J. B. Neilands. 1993. Isolation and structure of Rhizobactin 1021, a siderophore, from the alfalfa symbiont *Rhizobium meliloti* 1021. J. Am. Chem. Soc. 115: 3950 - 3956.

Ramirez-Bahena, M., Garcia-Fraile, P., Peix, A., Valverde, A., Rivas, R., Igual, J., Mateos, P., Martinez-Molina, E., and Velazquez, E. 2008. Revision of the taxonomic status of the species *Rhizobium leguminosarum* (Frank 1879) Frank 1889, *Rhizobium phaseoli* Dangeard 1926 and *Rhizobium trifolii* Dangeard 1926. *R. trifolii* is a later synonym of *R. leguminosarum*. Reclassification of the strain *R. leguminosarum* DSM 30132 (=NCIMB 11478) as *Rhizobium pisi* sp. nov. International Journal of Systematic and Evolutionary Microbiology. 58: 2484 - 2490.

Raymond, K. R., E. Dertz, and S. S. Kim. 2003. Enterobactin: an archetype for microbial iron transport. Proc. Natl. Acad. Sci. 100: 3584 - 3588.

Rozman, E., Albert, C., and Galceran, M.T. 2005. Ebrotidine and its metabolites studied by mass spectrometry with electrospray ionization. Comparison of tandem and in-source fragmentation. Rapid Communications in Mass Spectrometry. 9(15): 1492 – 1498.

Schwyn, B., and J. B. Neilands. 1987. Univeral chemical assay for the detection and determination of siderophores. Anal. Biochem. 160: 47 - 56.

Small, S., Puri, S., and O'Brian, M. 2009. Heme-dependent metalloregulation by the iron response regulator (Irr) protein in *Rhizobium* and other Alpha-proteobacteria. Biometals. 22: 89 - 97.

Smith, M. J., J. N. Shoolery, B. Schwyn, I. Holden, and J. B. Neilands. 1985. Rhizobactin, a structurally novel siderophore from *Rhizobium meliloti*. J. Am. Chem. Soc. 107: 1739 - 1743.

Stevens, J. B., R. A. Carter, H. Hussain, K. C. Carson, M. J. Dilworth, and A. W. B. Johnston. 1999. The fhu genes of *Rhizobium leguminosarum*, specifying siderophore uptake proteins: fhuDCB are adjacent to a pseudogene version of fhuA. Microbiol. 145: 593 - 601.

Storey E. 2005. Characterization of a Dihydroxamate-Type Siderophore Produce by *Rhizobium leguminosarum* IARI 917: Is It Schizokinen? M. S. Thesis. East Tennessee State University, Johnson City, TN.

Storey, E. P., Boghozian, R., Little, J. L., Lowman, D. W., Chakraborty, R. 2006. Characterization of "schizokinen"; a dihydroxamate-type siderophore produced by *Rhizobium leguminosarum* IARI 917. Biometals. 19(6): 637 - 649.

Streeter, J. 1985. Accumulation of α,α-Trehalose by *Rhizobium* bacteria and bacteroids. 164(1): 78 - 84.

Todd, J. D., M. Wexler, G. Sawers, K. H. Yeoman, P. S. Poole, and A. W. B. Johnston. 2002. RirA, an iron-responsive regulator in the symbiotic bacterium *Rhizobium leguminosarum*. Microbiol. 148: 4059 - 4071.

Verma, D. P. S., and S. Long. 1983. The molecular biology of Rhizobium-legume symbiosis. Intern. Rev. Cytology Suppl. 14: 211 - 245.

Viguier, C., P. O. Cuiv, P. Clarke, and M. O'Connell. 2005. RirA is the iron response regulator of the rhizobactin 1021 biosynthesis and transport genes in *Sinorhizobium meliloti*. FEMS Microbiol. Lett. 246: 235 - 242.

Weir, B.S. 2009. The current taxonomy of rhizobia. New Zealand rhizobia website. http://www.rhizobia.co.nz/taxonomy/rhizobia.html. Last updated: 14th September, 2009.

Wexler, M., Todd, JD, Kolade, O, Bellini, D, Hemmings, AM, Sawers, G, and Johnston, A. W. B. 2003. *Fur* is not the global regulator of iron uptake genes in *Rhizobium leguminosarum*. Microbiology. 149: 1357 - 1365.

Yeoman, K. H., Wisniewski-Dye, F., Timony, C., Stevens, J., deLuca, N., Downie, J., and Johnston, A. 2000. Analysis of the *Rhizobium leguminosarum* siderophore-uptake gene fhuA: differential expression in free-living bacteria and nitrogen-fixing bacteroids and distribution of an fhuA pseudogene in different strains. Microbiology. 146: 829 – 837.

Young et al. 2006. The genome of *Rhizobium leguminosarum* has recognizable core and

accessory components. Genome Biology. 7: R34.

APPENDIX

Additional Figures

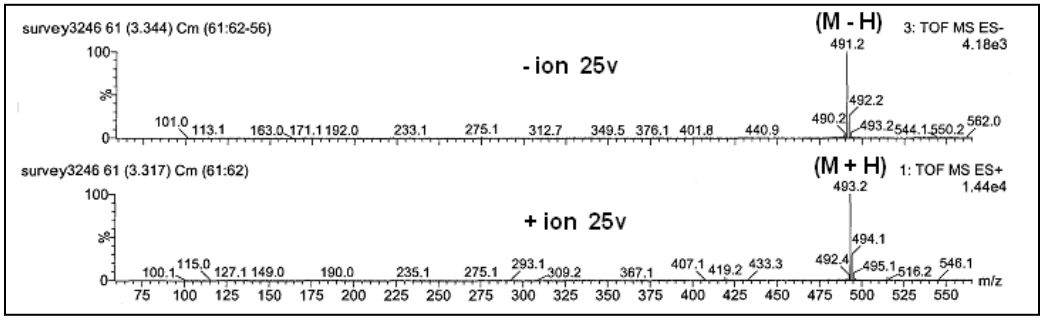

Figure 29: 25 v ES/MS spectra for iron-free siderophore "A" in both negative (top) and positive ion (bottom) modes. The marked major peaks indicate the molecular weight of the compound +/- one proton.

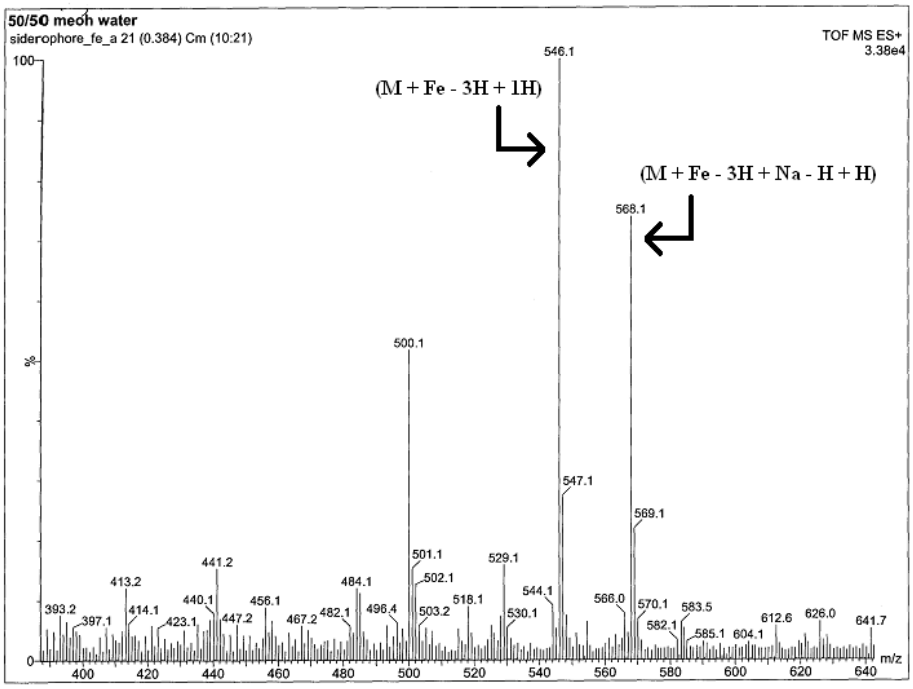

Figure 30: 25 v ES/MS spectra for iron-bound siderophore "A" in positive ion mode. The marked major peaks indicate the molecular weight of the ferric-compound both with and without a sodium (Na) adduct.

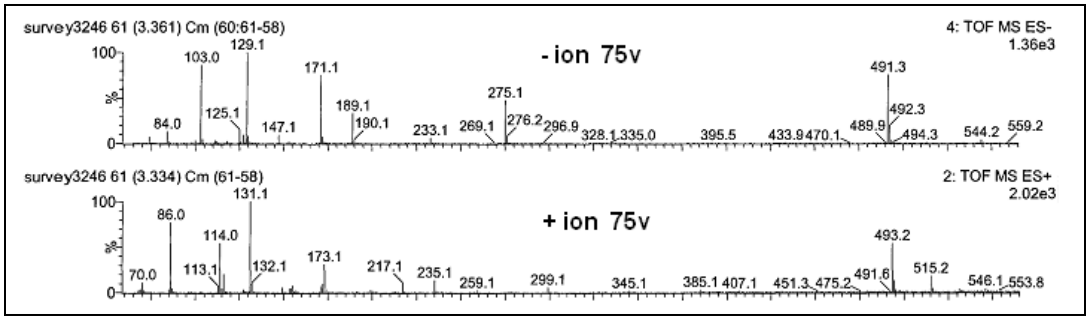

Figure 31: 75 v ES/MS fragmentation spectra for iron-free siderophore "A" in both negative (top) and positive ion (bottom) modes.

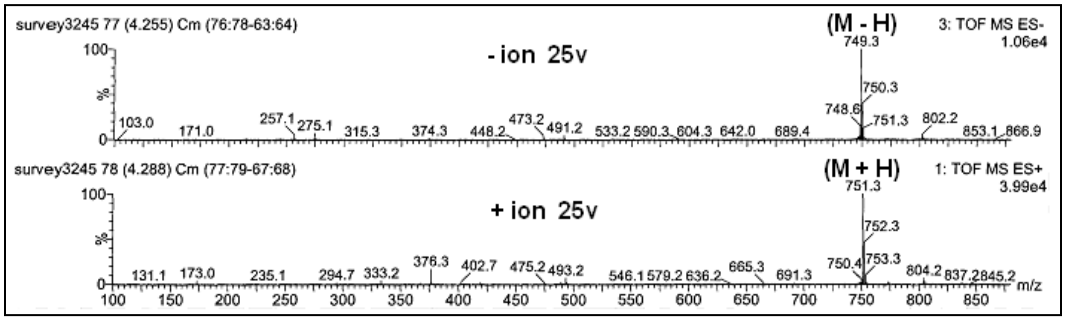

Figure 32: 25 v ES/MS spectra for iron-free siderophore "B" in both negative (top) and positive ion (bottom) modes. The marked major peaks indicate the molecular weight of the compound +/- one proton.

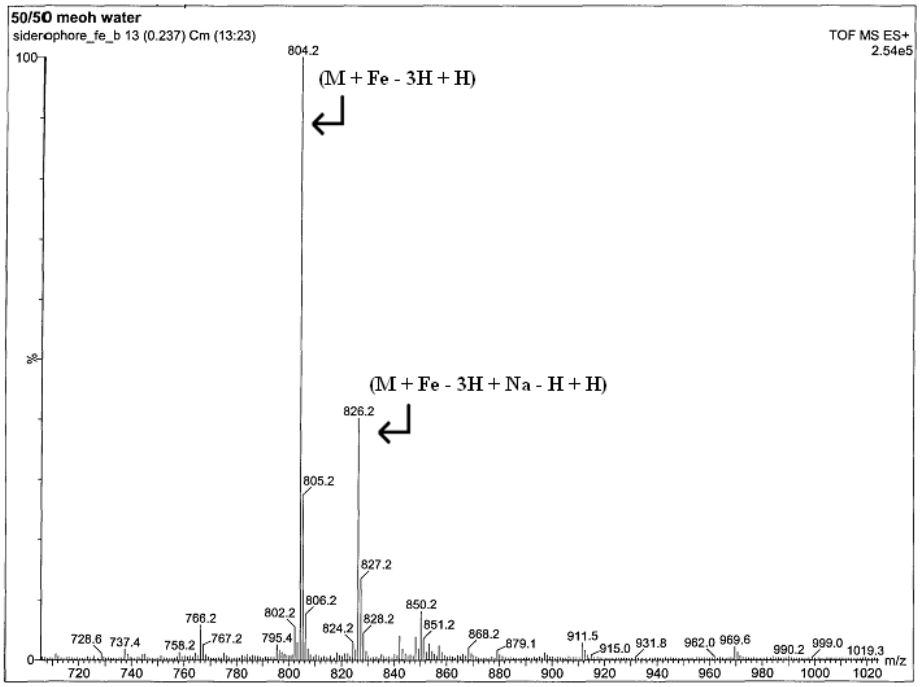

Figure 33: 25 v ES/MS spectra for iron-bound siderophore "B" in positive ion mode. The marked major peaks indicate the molecular weight of the ferric-compound both with and without a sodium (Na) adduct.

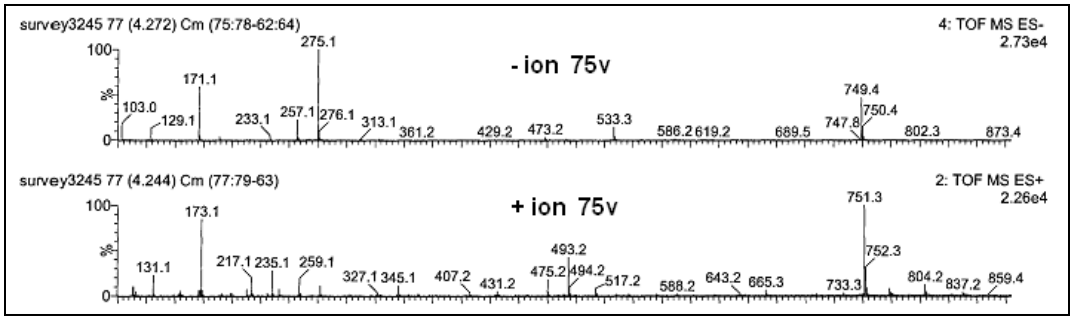

Figure 34: 75 v ES/MS fragmentation spectra for iron-free siderophore "B" in both negative (top) and positive ion (bottom) modes.

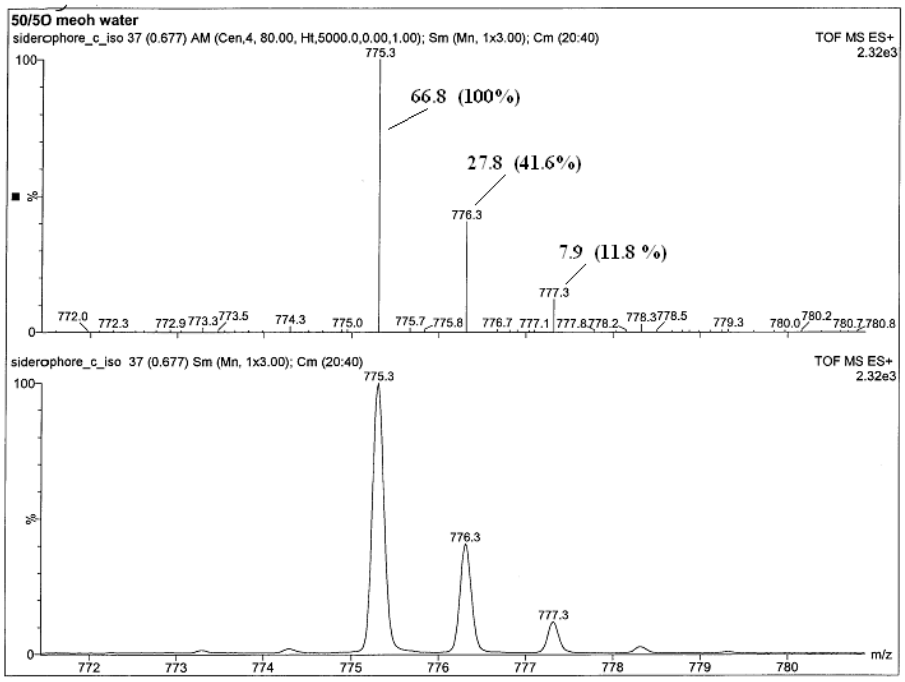

Figure 35: Experimentally determined carbon isotope ratios for compound "C".

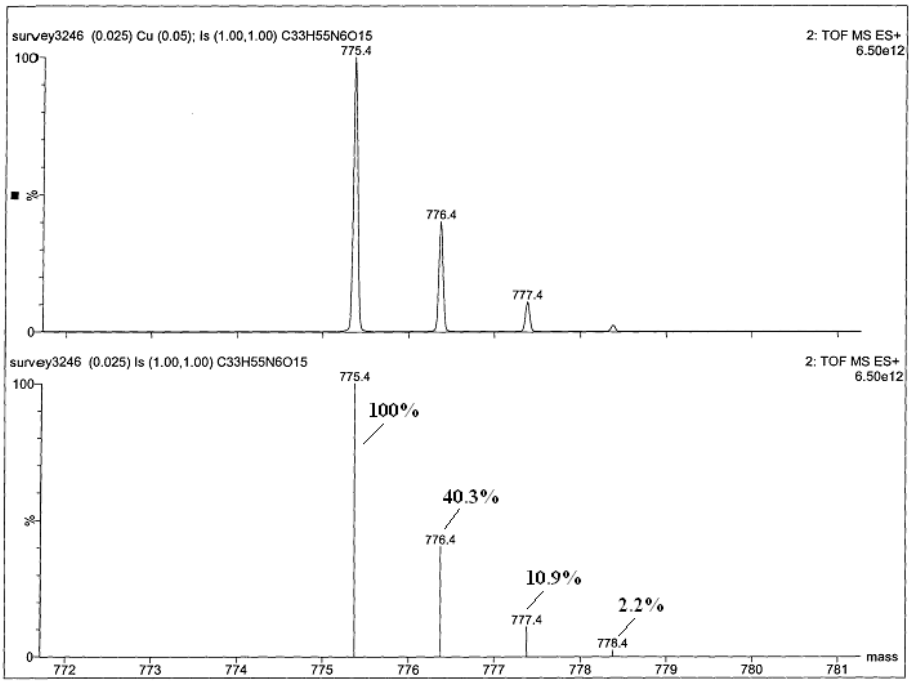

Figure 36: Theoretical carbon isotope ratios for $C_{33}H_{55}N_6O_{15}$, the chemical formula proposed for compound "C" by the Waters Elemental Composition report.

VITA

WILLIAM H. WRIGHT IV

Personal Data:	Date of Birth: September 29, 1979 Place of Birth: Johnson City, Tennessee Marital Status: Married
Education:	David Crockett High School, Jonesborough, Tennessee 1997 A.S., Northeast State Technical Community College, Blountville, Tennessee 2001 B.S. Biology, East Tennessee State University, Johnson City, Tennessee 2003 M.S. Biology conc. Microbiology, East Tennessee State University, Johnson City, Tennessee 2010
Professional Experience:	Graduate Assistant, East Tennessee State University, College of Public Health, 2007 – 2010 Laboratory Tech, East Tennessee State University, College of Public Health, 2009 – Present
Presentations:	Hammond, D. J., Storey, E., Wright, W., Lampson, B.C., Chakraborty, R. N. (2008). "Characterization of the Genes Involved in the Biosynthesis and Transport of Schizokinen, a Dihydroxamate Type Siderophore Produced by *Rhizobium leguminosarum* IARI 917." Abstract, 108th General Meeting of the American Society for Microbiology in Boston, MA. Hammond, D. J., Storey, E., Wright, W., Lampson, B.C., Chakraborty, R. N. (2008). "Characterization of the Genes Involved in the Biosynthesis and Transport of Schizokinen, a Dihydroxamate Type Siderophore Produced by *Rhizobium leguminosarum* IARI 917." Abstract, Appalachian Research Forum in Johnson City, TN.

Hammond, D. J., Storey, E., Wright, W., Lampson, B.C., Chakraborty, R. N. (2007). "Characterization of the Genes Involved in the Biosynthesis and Transport of Schizokinen, a Dihydroxamate Type Siderophore Produced by *Rhizobium leguminosarum* IARI 917." Abstract, 107th General Meeting of the American Society for Microbiology in Toronto, Ontario.

Hammond, D. J., Storey, E., Wright, W., Lampson, B.C., Chakraborty, R. N. (2007). "Characterization of the Genes Involved in the Biosynthesis and Transport of Schizokinen, a Dihydroxamate Type Siderophore Produced by *Rhizobium leguminosarum* IARI 917." Abstract, Appalachian Research Forum in Johnson City, TN.

Wright, W., Hammond, D. J., Storey, E., Lampson, B.C., Chakraborty, R. N. (2008). "Initial Identification of the Genes Involved in the Biosynthesis and Transport of Schizokinen, a Siderophore Produced by *Rhizobium leguminosarum* IARI 917." Abstract, Appalachian Research Forum in Johnson City, TN.

Preparation:

Wright, W. 2010. Isolation and Identification of the Siderophore "Vicibactin" Produced by *Rhizobium leguminosarum* ATCC 14479. M.S. Thesis. East Tennessee State University, Johnson City, TN.